Regulation of insulin signaling in Drosophila melanogaster

A DISSERTATION
SUBMITTED TO THE FACULTY
OF THE GRADUATE SCHOOL
OF THE UNIVERSITY OF MINNESOTA
BY

Jung Kim

IN PARTIAL FULFILLMENT OF THE REQUIREMENTS
FOR THE DEGREE OF
DOCTOR OF PHILOSOPHY

Adviser
Thomas P. Neufeld, PhD

August 2015

Abstract

Secreted ligands of the insulin family promote cell growth and maintain sugar homeostasis. Insulin release is tightly regulated in response to dietary conditions, but how insulin producing cells (IPCs) coordinate their responses to distinct nutrient signals is unclear. Here I show that regulation of insulin secretion in Drosophila larvae has been segregated into distinct branches: circulating sugars selectively promote the release of Drosophila insulin-like peptide 3 (Dilp3), whereas amino acids selectively promote secretion of Dilp2. Dilp3 is uniquely required for sugar-mediated activation of TOR signaling and suppression of autophagy in the larval fat body. Sugar levels are not sensed directly by the IPCs, but rather by the adipokinetic hormone (AKH)-producing cells of the corpora cardiaca, and I demonstrate that AKH signaling is required in the IPCs for sugar-dependent Dilp3 release. Thus, IPCs integrate multiple cues to regulate secretion of distinct insulin subtypes under varying nutrient conditions.

The sensitivity of insulin signaling determines the activity of insulin in the presence of insulin, and misregulation of insulin sensitivity leads to metabolic diseases such as type-2 diabetes. Mechanical stress is a known regulator of insulin sensitivity, but the mechanisms by which mechanical stress regulates insulin sensitivity are unclear. Here, I showed that mechanical stress is required for activation of insulin signaling in the Drosophila larval fat body both *ex vivo* and *in vivo*. Interestingly, mechanical stress affects most of components in the insulin pathway: localization of insulin receptor (InR), chico, and lnk, and the activities of PI3K, AKT, and TOR. I demonstrated that integrin signaling, previously shown to sense mechanical stress, is necessary for the insulin- and mechanical stress-dependent activation of TOR. Together, my data suggest that mechanical stress sensed by integrin signaling regulates insulin sensitivity by altering upstream components of insulin signaling, such as InR, chico and lnk.

Table of Contents

List of Figures

List of Abbreviations

AKH	adipokinetic hormone
ATG1	autophagy related protein 1
CC	corpora cardiaca
Dilps	Drosophila insulin-like peptides
ECM	extra cellular matrix
GLP-1	glucagon-like peptide 1
GLUT	glucose transporter
GPCR	G protein coupled receptor
IGF-1R	insulin-like growth factor-1 receptor
InR	insulin receptor
Ins	insulin
IPCs	insulin producing cells
PH domain	pleckstrin homology domain
PIP2	phosphatidylinositol 2-phosphate
PIP3	phosphatidylinositol 3-phosphate
PI3K	phosphoinositide 3-kinase
PTEN	phosphatase and tensin homolog
RTK	receptor tyrosine kinase
S6K	ribosomal protein S6 kinase
tGPH	tubulin promoter: GFP-PH domain
tobi	target of brain insulin
TOR	target of rapamycin
TSC 1/2	tuberous sclerosis complex 1/2
Tub	tubulin
T1D	type-1 diabetes
T2D	type-2 diabetes
Vkg	viking
4EBP	eukaryotic translation initiation factor 4E binding protein

CHAPTER 1: Introduction

Insulin

Insulin is an essential peptide hormone regulating sugar homeostasis in the blood (Matteucci et al., 2015). Insulin is produced in the beta cells of the mammalian pancreas and stored in the insulin granules. When the glucose level in the blood is increased, pancreatic beta cells release insulin, which promotes uptake of glucose in peripheral organs of the body such as muscles, liver, and fat. Because of its pivotal role in sugar homeostasis, insulin is tightly linked to diabetes, which is a metabolic disorder causing hyperglycemia, a condition showing abnormally elevated glucose level in the blood. Glucose is an essential source of carbohydrate generating energy in organisms, whereas elevated level of glucose can be harmful to the body (Yan, 2014). Glucose can cause abnormal glycation of protein or lipids, changing their stability and functions. Glucose metabolism (glycolysis) can also alter energy metabolism in many tissues. Thus, the glucose level in the blood must be tightly regulated and insulin is the key hormone for this regulation.

Diabetes is categorized into two subtypes: Type-1 diabetes (T1D) and Type-2 diabetes (T2D) (Cnop et al., 2005; Simmons and Michels, 2015). In T1D, the level of circulating insulin in the blood is not properly regulated. Failure of the pancreatic beta cell function, which results from autoimmune reaction, leads to a shortage of insulin in the blood. On the other hand, T2D is triggered by chronic uptake of excessive dietary nutrition, which causes hyperinsulinemia, a condition of abnormally elevated insulin in the blood. Without proper treatment, hyperinsulinemia develops insulin resistance in the peripheral tissues, leading to defective insulin signaling even with the elevated level of insulin in the blood. These tissues, which are insensitive to insulin, are unable to uptake

enough glucose, which in turn, promotes more secretion of insulin from pancreatic beta cells. This vicious cycle of hyperinsulinemia and hyperglycemia exhausts pancreatic beta cells and eventually causes their apoptotic cell death.

Since diabetes is one of the major growing health problems in modern society (Egger and Dixon, 2014), it is important to better understand how insulin works. Establishment of a model system that recapitulates the properties of insulin signaling in humans could be useful to develop new therapeutic treatments for diabetes.

Insulin signaling

Secreted insulin in the blood activates insulin signaling, which is a conserved mechanism in metazoans, in the peripheral tissues (Gong et al., 2014). Insulin triggers activation of insulin receptor (InR), a member of the receptor tyrosine kinase (RTK) family, by auto-phosphorylation. Activated InR recruits the adapter proteins, such as IRS-1 and Lnk, to activate phosphoinositide 3-kinase (PI3K) (Fig. 1). In turn, PI3K converts phosphatidylinositol 2-phosphate (PIP2) to phosphatidylinositol 3-phosphate (PIP3) at the plasma membrane. PIP3 recruits proteins containing pleckstrin homology domain (PH domain), such as Phosphatase and tensin homolog (PTEN), a PIP3 phosphatase, counteracts the activity of PI3K. Subsequently, AKT, a PH domain-containing serine / threonine- kinase, is recruited to PIP3 on the membrane and activated. AKT relays insulin signaling through inhibition of tuberous sclerosis complex 1/2 (TSC1/2). In addition, activated AKT promotes translocation of glucose transporter (GLUT) to the membrane, leading to the uptake of glucose from the blood (Hajiaghaalipour et al., 2015). Reduced activity of TSC 1/2 liberates activation of the small GTPase Rheb, a positive

Figure 1

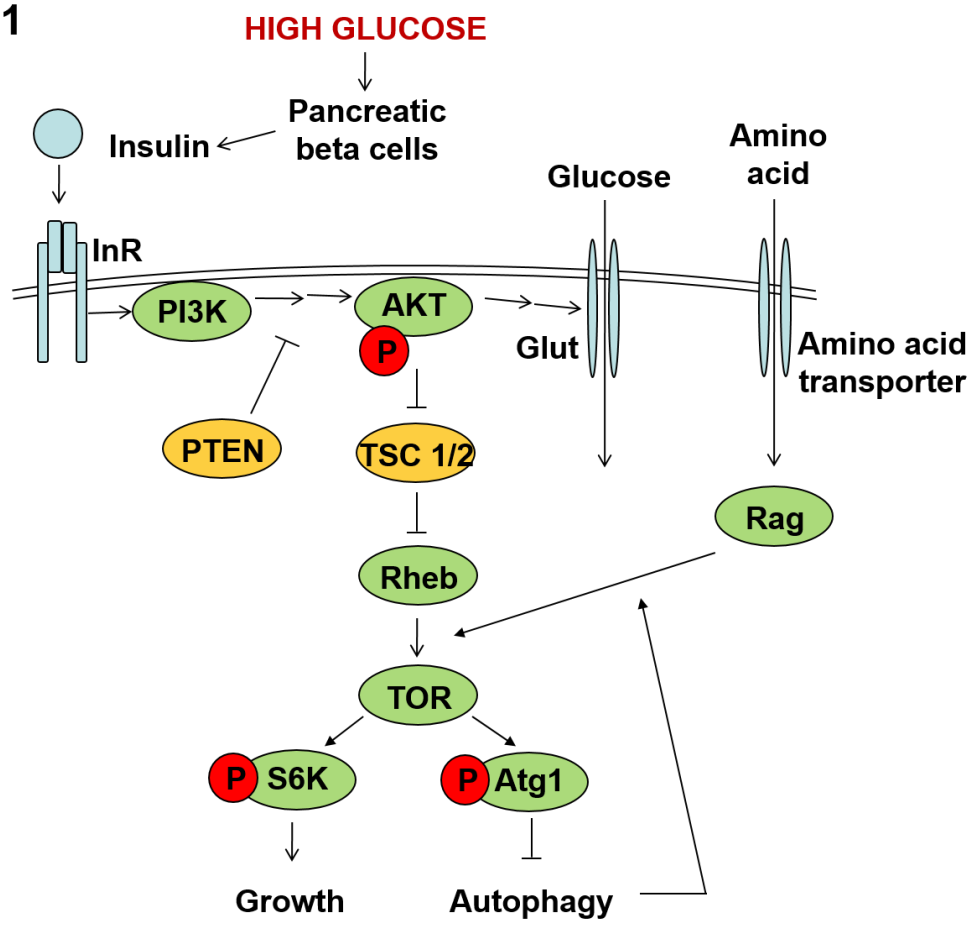

Figure 1. A cartoon representing insulin signaling in mammals.

regulator of target of rapamycin (TOR), which is a crucial serine / threonine kinase for regulating growth and development. TOR phosphorylates multiple targets, such as ribosomal protein S6 kinase (S6K) and eukaryotic translation initiation factor 4E binding protein (4EBP) (Johnson et al., 2013). Phosphorylation of these proteins enhances translation of mRNAs, which promotes cell growth.

Because of the anabolic functions of insulin signaling, diminished insulin signaling caused by mutations can lead to severe growth and developmental defects in humans. Mutations in InR cause Donohue syndrome or Rabson-Mendenhall syndrome, which are genetic disorders leading to growth retardation (Bathi et al., 2010; Musso et al., 2004). Hyper activation of insulin signaling is well observed in many cancers. Mutations of PTEN increase the chance of tumorigenesis in a large number of cancers (Azim et al., 2010), and mutations of TSC1 or TSC2 cause Tuberous Sclerosis, which is a genetic disease leading to benign tumors (DiMario et al., 2015). Thus, insulin signaling has been a therapeutic target for cancer (Beauchamp and Platanias, 2013; Feitelson et al., 2015).

By phosphorylation of autophagy related protein 1 (ATG1), activated TOR inhibits autophagy, which is a catabolic mechanism generating an alternative source of nutrients under starvation conditions (Chang and Neufeld, 2010). Cytoplasmic compartments are engulfed by double-membrane structure, called an autophagosome. Subsequently, autophagosomes fuse with lysosomes to form autolysosomes, which degrade contents inside using lysosomal digestive enzymes, such as cathepsins, and supply nutrition back to the cell under starvation.

Autophagy is closely related to human diseases because of its functions in removal of damaged organelles and misfolded proteins, which are sequestered and

degraded in autolysosomes (Ciechanover and Kwon, 2015). Defects of autophagy in the brain promotes accumulation of misfolded protein aggregates, which cause neurodegenerative diseases such as Huntington's, Alzheimer's, and Parkinson's diseases.

Altogether, these essential functions of insulin signaling in human health highlight the need for a more thorough investigation of how insulin signaling is regulated.

Regulation of insulin signaling

The amount of insulin in the blood is the major determinant of the activity of insulin signaling in peripheral tissues, and it is regulated by production and secretion of insulin. Production and maturation of insulin occurs in the pancreatic beta cell (Matteucci et al., 2015). Preproinsulin, a long peptide containing signal sequence, chain A, B, and C, is produced and packed in the insulin granules. By removal of its signal sequence, preproinsulin is processed into proinsulin, the intermediate containing two disulfide bonds between chain A and B, and one disulfide bond between cysteines in chain A. After cutting out chain C, the mature form of insulin is produced.

Secretion of insulin granules is regulated by the ATP-sensitive potassium channel (Rorsman and Braun, 2013). Pancreatic beta cells absorb glucose from the blood and convert it into ATP through the TCA cycle. The elevated level of ATP leads to closure of the ATP-sensitive potassium channel, which depolarizes the plasma membrane. Subsequently, the voltage-dependent calcium channel is opened, causing secretion of insulin, which then activates insulin signaling in peripheral tissues.

Cross-talk with other pathways is also important for insulin signaling. Pancreatic alpha cells synthesize the proglucagon peptide, which is processed into multiple mature

peptide hormones, mainly glucagon (Ahren, 2015; Moon and Won, 2015). Low level of glucose in the blood stimulates pancreatic alpha cells to secrete glucagon, which activates the glucagon receptor, a member of G protein coupled receptors (GPCR), in the liver. By stimulating gluconeogenesis as well as glycogenolysis, in which the liver converts stored carbohydrates into glucose, glucagon signaling leads to an increase in blood sugar levels. For fine tuning of sugar homeostasis, insulin and glucagon give negative feedback to each other.

The intestinal cells produce and process the proglucagon peptide into glucagon-like peptide-1 (GLP-1), which has opposite functions to glucagon (Baggio and Drucker, 2007; Heppner and Perez-Tilve, 2015). GLP-1 suppresses appetite and slows down emptying the gut. In addition, GLP-1 promotes proliferation of pancreatic beta cells, production and secretion of insulin. Because of its beneficial effects on insulin signaling, GLP-1 is highlighted as a therapeutic material for diabetic patients.

Amino acids also play an important role in insulin signaling, by promoting activation of TOR (Jewell et al., 2013). Cellular amino acids stimulate conversion of the small GTPase Rag to its GTP-bound form, which recruits TOR to the membrane of lysosomes, where Rheb is constitutively located. In turn, Rheb triggers activation of TOR. This mechanism also explains how autophagy gives positive feedback to TOR (Yu et al., 2010). The low activity of TOR under starvation induces autophagy, which generates amino acids by degradation of cytoplasmic proteins. Released amino acids from autolysosomes reactivate TOR and turn off autophagy.

Mechanical stress can also affect the activity of RTK signaling in specific tissues. Cells in the bone, blood vessels, or muscles sense mechanical stress, which stimulates

integrin signaling (Tahimic et al., 2013). Integrins are located in the membrane of the cell and link the extra cellular matrix (ECM) to the cells (Harburger and Calderwood, 2009). Mechanical load in bones cells triggers activation of integrin, which forms a cluster with insulin-like growth factor-1 receptor (IGF-1R) (Saegusa et al., 2009). This integrin/IGF-1R cluster increases sensitivity of IGF-1R to IGF-1 (Long et al., 2011), but the mechanism underlying this is not fully understood.

Insulin signaling in Drosophila

Drosophila melanogaster has been used for decades as a model system to understand the mechanism of human disease (Pandey and Nichols, 2011; Schneider, 2000). Useful tools of genetics, cell biology and molecular biology have made Drosophila a strong *in vivo* model organism. Completed genome sequencing, fast generation time, large number of progeny, low expense and ease of handling are advantages of Drosophila. However, the use of Drosophila as a model system for understanding human diabetes is relatively new (Teleman et al., 2012).

Although most components of insulin signaling are conserved between humans and Drosophila, there are some important differences between these systems. Insects including Drosophila use trehalose, a disaccharide composed of two glucoses, as the major sugar in circulating fluid, called hemolymph (Becker et al., 1996). Drosophila maintains 10-fold higher concentration of trehalose than the concentration of glucose in humans. This high concentration is not harmful, since trehalose is a non-reactive sugar.

Another unique feature of Drosophila is the presence of multiple insulin-like peptides (Dilps), which serve homologous functions to human insulin such as sugar

homeostasis (Ikeya et al., 2002). Eight Dilps have been identified, and among them Dilp2, 3, and 5 are expressed in the insulin producing cells (IPCs) in the larval brain (Colombani et al., 2012; Gronke et al., 2010). Knockout of multiple Dilps or genetic ablation of IPCs leads to elevated trehalose in the hemolymph and severe growth defects, which mimic the conditions in human T1D (Rulifson et al., 2002). However, the mechanism of production and secretion of Dilps is still unclear. Whereas glucose regulates secretion of insulin in mammals, dietary amino acids, not trehalose, stimulate secretion of Dilp2 from the IPCs (Geminard et al., 2009). The larval fat body, which is a homologous organ to the liver and adipose tissues in mammals, senses dietary amino acids and produces an uncharacterized signal that promotes Dilp2 secretion into the hemolymph under conditions of nutrient sufficiency. In adult flies, the fat body secretes the JAK/STAT ligand Unpaired 2 in response to dietary nutrients, which also stimulates Dilp2 release (Rajan and Perrimon, 2012). Whether secretion of other Dilps is controlled through similar mechanisms is unclear, and the direct effects of hemolymph sugar levels on Dilp release remain poorly understood.

Cross-talk between insulin signaling and other pathways is not characterized completely in the fly system. Adipokinetic hormone (AKH), which is produced in the corpora cardiaca (CC) in the ring gland, has homologous functions to glucagon (Kim and Rulifson, 2004; Lee and Park, 2004). Genetic ablation of the CC causes hypoglycemia, which is similar to defects of glucagon signaling in humans. It is, however, still unclear whether and how insulin signaling and AKH signaling affect each other.

Interactions between InR and integrin signaling are uncharted territories in Drosophila. Drosophila has homologous players in the integrin pathway: integrin alpha

and beta subunits, and integrin binding proteins such as talin, linking integrin to the actin cytoskeleton (Lowell and Mayadas, 2012). The mechanisms of integrin signaling have been well studied, but potential cross-talk between integrin and insulin signaling is unclear.

Aims of the thesis

Filling the gap of knowledge in insulin signaling between humans and fruit flies would be a critical step to establish Drosophila as a model system for diabetes. In my thesis work, I focused on the effect of sugar on Dilp secretion and mechanical stress regulating sensitivity of InR to insulin.

In Chapter 2, I show that Dilp2 and Dilp3 differ in their regulation by distinct classes of nutrients: whereas Dilp2 secretion responds selectively to amino acids, secretion of Dilp3 is stimulated primarily by glucose and trehalose, the major sugar present in Drosophila larval hemolymph. Further, I demonstrate that trehalose stimulates the CC to release AKH, which then acts directly on the IPCs to promote secretion of Dilp3. Trehalose-mediated Dilp3 secretion from the IPCs leads to upregulation of TOR signaling and suppression of autophagy in the larval fat body, and is required for sugar homeostasis and normal rates of larval development under nutritional stress. I propose that coupling AKH release to the selective secretion of Dilp3 plays a critical role in promoting sugar homeostasis under the conditions of high insulin signaling required for rapid cell growth during larval development.

In Chapter 3, I show that mechanical stress is required for TOR activation in the fat body *ex vivo*, and crawling body movement is necessary for TOR activation *in vivo*.

Multiple components in the insulin signaling pathway from InR to TOR are regulated by mechanical stress. Through RNAi screening I identified collagen IV in the ECM, integrin beta PS, and talin as required for maintaining association of fat body cells and activation of insulin signaling.

CHAPTER 2: Dietary sugar promotes systemic TOR activation in Drosophila through AKH-dependent selective secretion of Dilp3

Note to readers: This chapter was published in the journal *Nature Communications* 6:6846, 2015. In recognition that this work involved collaboration between the authors, this chapter uses the first person plural ("we") instead of first person singular ("I"). Individual contributions to this work are described in APPENDIX. Nature Publishing Group allows authors to reproduce articles for their thesis without permission. Refer to http://www.nature.com/reprints/permission-requests.html for more details.

Trehalose promotes activation of TOR in the larval fat body

To examine how systemic insulin signaling activity is influenced by sugar levels in Drosophila larvae, we developed an e*x vivo* culture system in which dissected larval carcasses are incubated in media with varying sugar concentrations. As a measure of insulin signaling in peripheral tissues, we first examined the activity of TOR in the larval fat body, a site of high sensitivity to insulin signaling. Incubation of inverted larval carcasses in M3 media, which contains a complete mixture of essential amino acids and a low concentration of sugar (10 mg/ml glucose), led to a rapid decrease in TOR-dependent phosphorylation of S6K Thr398 in fat body extracts (Fig. 2-1a). We refer hereafter to this phosphorylation signal as fb-TOR activity. In contrast, fb-TOR activity was maintained when M3 media was supplemented with glucose or trehalose, the two main sugars present in Drosophila hemolymph (Fig.2-1a, Fig. 2-2a, b). Sucrose, which is not a constituent of hemolymph, did not support fb-TOR activity (Fig. 2-2b). As trehalose, but not glucose, promoted fb-TOR activity in the range of its normal physiological concentration in larval hemolymph (Tennessen et al., 2014), we focused our further analysis on this disaccharide.

The effects of trehalose *ex vivo* were recapitulated in *in vivo* feeding experiments. Larvae raised on agar/tryptone food containing trehalose showed dose-dependent activation of TOR in the fat body compared to food lacking trehalose (Fig. 2-1a). As a physiological readout of this pathway, we monitored the effect of trehalose on induction of autophagy, which is inhibited by TOR signaling. Both *in vivo* feeding and *ex vivo* incubation in the absence of trehalose led to the formation of mCherry-Atg8-positive autophagosomes and autolysosomes throughout the larval fat body within four hours.

Figure 2-1

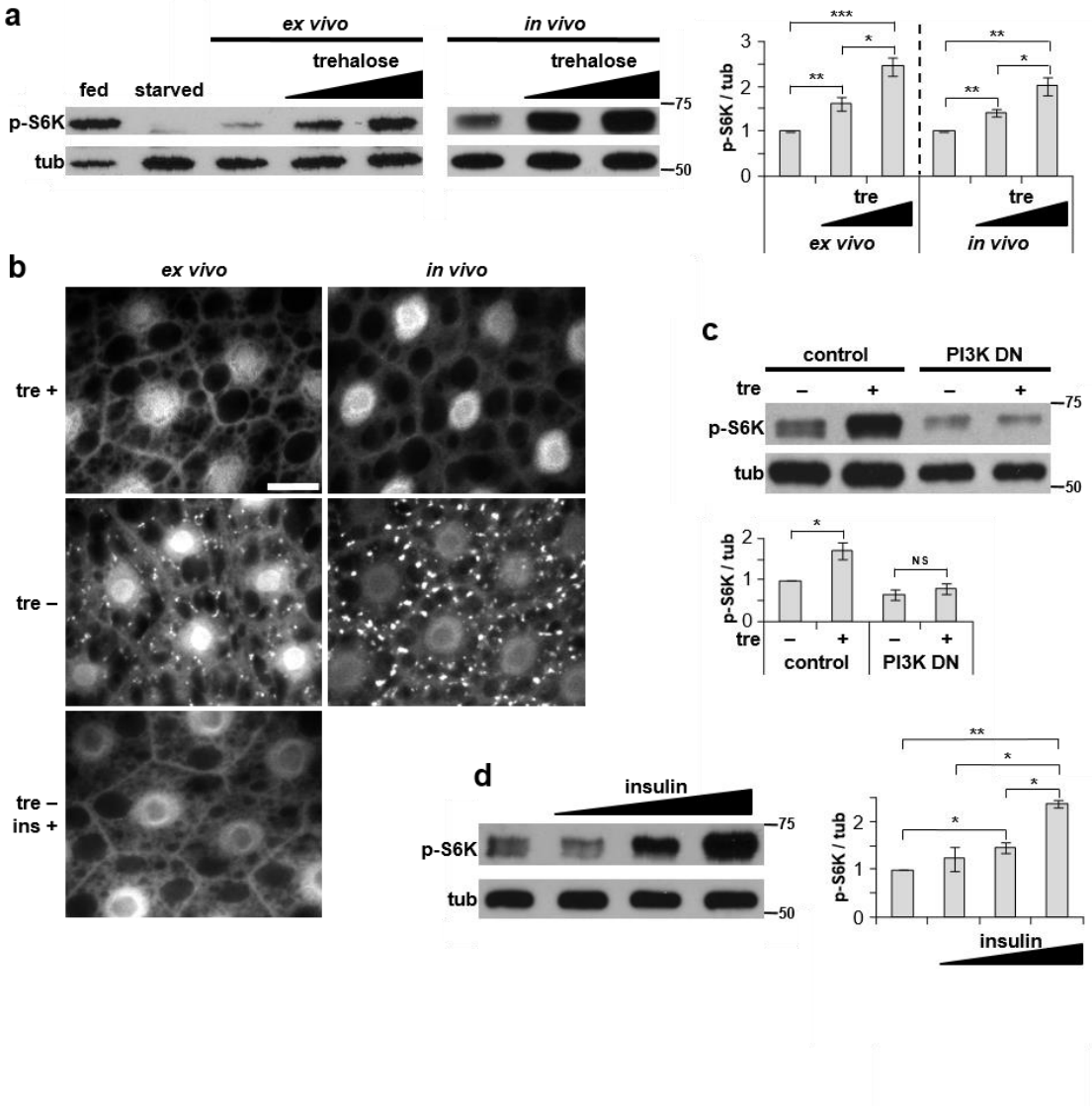
a
ex vivo
in vivo
trehalose
trehalose
fed
starved
p-S6K
tub
75
50
p-S6K / tub
tre
ex vivo
in vivo
b
ex vivo
in vivo
tre +
tre –
tre –
ins +
c
control
PI3K DN
tre
p-S6K
tub
NS
control
PI3K DN
d
insulin
p-S6K
tub
insulin

Figure 2-1: Trehalose promotes TOR signaling in the larval fat body.

(a) TOR activity was measured by immunoblot of wild type fat body extracts with phospho-T398 S6K (p-S6K) antibody. Fed and starved controls (lanes 1 and 2) show the range of fb-TOR activity on standard fly food and following 2-hr starvation. In both *ex vivo* (larval carcasses incubated 2 hours in M3 media with 0, 20 or 40 mg/ml trehalose) and *in vivo* (larvae cultured overnight in agar/tryptone food with 0, 13.3 or 26.6 mg/ml trehalose) cultures, addition of trehalose (tre) results in a dose-dependent increase in p-S6K. Data represent mean±s.e.m. of four independent experiments. **(b)** Trehalose inhibits formation of autophagic vesicles in larval fat body cells. *Cg-Gal4 / UAS-mCherry-Atg8a* carcasses or larvae were incubated under *ex vivo* (4 hr in M3 media +/-20 mg/ml trehalose) or *in vivo* (overnight on agar/tryptone food +/-26.6 mg/ml trehalose) conditions. Human insulin (10 µg/ml) inhibits autophagosome formation in *ex vivo* cultures lacking trehalose. Scale bar represents 20 µm. Images are representative of three experiments (seven larvae per condition). **(c)** PI3-kinase activity is required for *ex vivo* activation of fb-TOR by trehalose. Expression of dominant negative p110 catalytic subunit in the fat body *(Cg-GAL4 / UAS-p110^{D954A})* reduces fb-TOR activity and inhibits its response to trehalose. Data represent mean±s.e.m. of three independent experiments. **(d)** Addition of human insulin (0.01, 0.1, and 1 µg/ml) to *ex vivo* cultures lacking trehalose causes dose-dependent increases in fb-TOR activity. Data represent mean±s.e.m. of three independent experiments. Graphs display ratios of p-S6K/tubulin (tub) band intensities, normalized to control.*$p<0.05$, **$p<0.01$, ***$p<0.001$, NS $p>0.05$; Student's *t*-test.

Figure 2-2

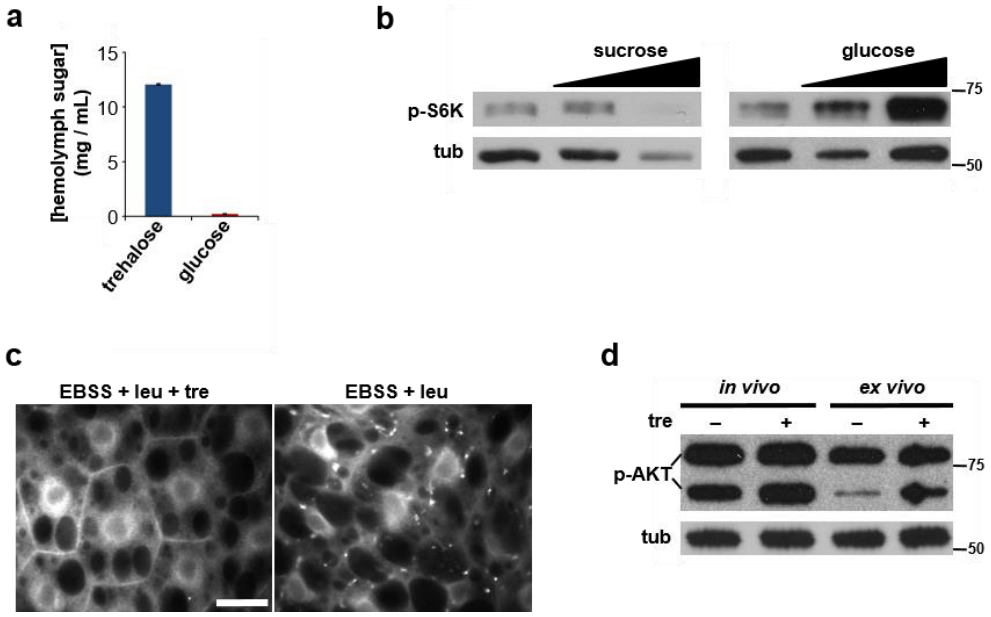
a
[hemolymph sugar] (mg / mL)
15
10
5
0
trehalose
glucose
b
sucrose
glucose
p-S6K
tub
75
50
c
EBSS + leu + tre
EBSS + leu
d
in vivo
ex vivo
tre
–
+
–
+
p-AKT
tub
75
50

Figure 2-2: Alternative *ex vivo* conditions and assays for fat body TOR activity. **(a**) *In vivo* levels of circulating trehalose and glucose in third instar larvae. **(b)** *Ex vivo* phosphorylation of S6K T398 in response to increasing concentration of sucrose or glucose (0, 20 or 40 mg/ml in M3 media). **(c)** Accumulation of mCherry-Atg8a punctae after 4 hrs *ex vivo* incubation in EBSS/leucine media with (left) and without (right) 20 mg/ml trehalose. Scale bar 20 µm. **(d)** Phosphorylation of AKT S505 is stimulated by trehalose *in vivo* (26.6 mg/ml in agar/tryptone food) and *ex vivo* (40 mg/ml in M3 media). Data in a, b, and d each represent three independent experiments. Images in c are representative of two trials each using seven carcasses per condition.

Inclusion of trehalose in these experiments prevented autophagy induction (Fig. 2-1b). *Ex vivo* incubation in a more severe starvation medium (EBSS supplemented with leucine) also led to autophagy induction that was suppressed by trehalose (Fig. 2-2c). Together, these data suggest that both dietary and circulating hemolymph trehalose can promote TOR activation in the larval fat body.

Trehalose regulates systemic insulin signaling

Several lines of evidence indicated that activation of TOR by trehalose may be mediated by insulin signaling. First, trehalose-dependent TOR activation was strongly inhibited by expression in the fat body of a dominant-negative PI3-kinase subunit, a central component of the insulin pathway (Fig. 2-1c). Second, the *ex vivo* requirement for trehalose to maintain fb-TOR activation and suppress autophagy was bypassed by inclusion of human insulin in the medium (Fig. 2-1b, d). Finally, trehalose promoted phosphorylation of Akt on Ser505, a site of activation regulated by insulin signaling (Fig. 2-2d).

Of the eight Drosophila insulin-like proteins, Dilp2, Dilp3 and Dilp5 are expressed in twin clusters of IPCs within the central nervous system. To examine the potential involvement of these brain-derived Dilps in mediating the systemic effects of trehalose, we first tested whether the CNS itself is required for trehalose-stimulated activation of TOR. Whereas trehalose promoted dose-dependent S6K phosphorylation in the fat body of complete carcasses, removal of the brain and associated ring gland complex abrogated this response (Fig. 2-3a). Trehalose also failed to suppress autophagy

Figure 2-3

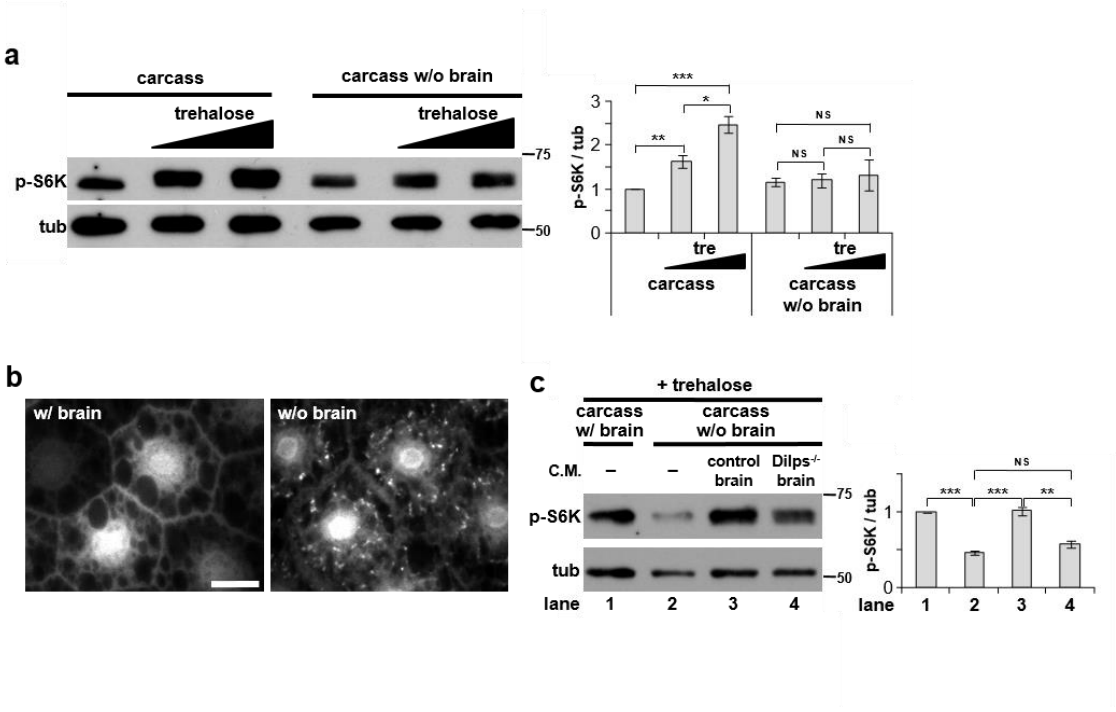
a
carcass
carcass w/o brain
trehalose
trehalose
p-S6K
tub
75
50
p-S6K / tub
***
*
**
NS
NS
NS
tre
carcass
tre
carcass w/o brain
b
w/ brain
w/o brain
c
+ trehalose
carcass w/ brain
carcass w/o brain
C.M.
–
–
control brain
Dilps-/- brain
p-S6K
tub
75
50
lane 1 2 3 4
p-S6K / tub
NS
***
***
**
lane 1 2 3 4

Figure 2-3: Trehalose-dependent activation of TOR in the larval fat body requires the brain and insulin signaling.

(a) Supplementation of M3 media with trehalose (0, 20, 40 mg/ml) leads to significant increases in fb-TOR activity from whole larval carcasses (left) but not in carcasses from which the brain was surgically removed (right).Data represent mean±s.e.m. of four independent experiments. **(b)** Trehalose (20 mg/ml in M3) suppresses formation of autophagic vesicles (mCherry-Atg8 punctae) in fat body cells of complete carcasses but not carcasses lacking the brain. Scale bar represents 20 µm. Representative images of three experiments (seven carcasses per condition). **(c)** Fb-TOR activity of carcasses lacking the brain, incubated in control M3+trehalose media (-), or in M3+trehalose conditioned media (C.M.) previously incubated 2h with CNS complexes from wild type larvae (control brain) or from mutant larvae lacking *Dilps1-5* and *Dilp7* ($Dilps^{-/-}$ brain).Data represent mean±s.e.m. of four independent experiments. *p<0.05, **p<0.01, ***p<0.001, NS p>0.05; Student's *t*-test.

induction in the fat body of brain-less larval carcasses (Fig. 2-3b). To ask whether soluble factors from the brain are released into the media, we pretreated M3+trehalose media by incubation with larval brain/ring gland complexes. This conditioned media was able to fully activate S6K phosphorylation in the fat body of brain-less carcasses (Fig. 2-3c). In contrast, media conditioned with CNS complexes from larvae mutant for *Dilps1-5* and *Dilp7* was significantly less effective in this assay. These results indicate that trehalose-dependent activation of TOR in the larval fat body is a non-autonomous response requiring a CNS-derived signal, and that one or more of the brain-derived Dilps are required for a significant portion of this signal.

Trehalose activates TOR via selective secretion of Dilp3

The requirement for the central nervous system implicates Dilp2, Dilp3 and/or Dilp5 in trehalose-responsive signaling. To directly test the potential role of these factors, we examined the effects of trehalose in mutant animals individually lacking each Dilp. Whereas homozygous *Dilp2* and *Dilp5* mutants each showed normal fat body TOR activation following *ex vivo* incubation in trehalose-containing media, this response was defective in *Dilp3* mutant larvae (Fig. 2-4a). Similarly, mutation of *Dilp3* but not *Dilp2* or *Dilp5* strongly reduced fb-TOR signaling *in vivo* in response to inclusion of trehalose in the diet (Fig. 2-4b). Thus, we conclude that trehalose elicits systemic insulin signaling primarily through Dilp3.

Géminard and coworkers showed previously that dietary amino acids promote secretion of Dilp2 from the IPCs, and that Dilp2 protein accumulates to high levels in these cells in response to amino acid starvation (Geminard et al., 2009). We used a

Figure 2-4

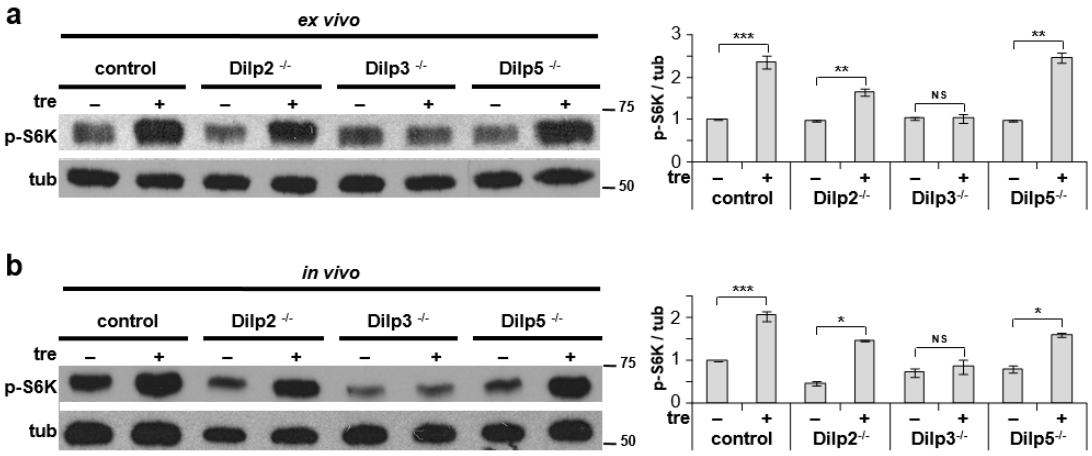
a
ex vivo
control
Dilp2 -/-
Dilp3 -/-
Dilp5 -/-
tre
– + – + – + – +
p-S6K
tub
75
50
p-S6K / tub
***
**
NS
**
tre
control
Dilp2-/-
Dilp3-/-
Dilp5-/-
b
in vivo
control
Dilp2 -/-
Dilp3 -/-
Dilp5 -/-
tre
– + – + – + – +
p-S6K
tub
75
50
p-S6K / tub
***
*
NS
*
tre
control
Dilp2-/-
Dilp3-/-
Dilp5-/-

Figure 2-4: Dilp3 is required for TOR activation by trehalose.

(a) *Ex vivo* incubation of larval carcasses in M3 media supplemented with or without 40 mg/ml trehalose. Trehalose promotes fb-TOR activity in control, *Dilp2*$^{-/-}$ and *Dilp5*$^{-/-}$ larvae, but not in *Dilp3*$^{-/-}$ larvae. **(b)** *In vivo* incubation of larvae in agar/tryptone food containing 0 or 26.6 mg/ml trehalose. Fb-TOR activity is significantly increased by trehalose in control, *Dilp2*$^{-/-}$ and *Dilp5*$^{-/-}$ larvae, but not in *Dilp3*$^{-/-}$ larvae. Representative blots of three independent experiments are shown in each panel. Data were assessed by Student's *t*-test and are represented as mean±s.d. *$p<0.05$, **$p<0.01$, ***$p<0.001$, NS $p>0.05$.

similar immunostaining approach to examine the effects of trehalose on Dilp accumulation and release. Following *ex vivo* incubation in M3 media supplemented with trehalose, protein levels of both Dilp2 and Dilp3 were low in the IPCs, as assayed by antibodies specific for either Dilp2 or Dilp3 (see Fig. 2-5a,b for antibody control experiments). In contrast, incubation in media lacking trehalose led to a marked accumulation of Dilp3 but not Dilp2 in these cells (Fig. 2-6a). Similar effects were observed *in vivo*: staining intensity of both Dilps was low in the IPCs of larvae raised on food rich in amino acids and trehalose, and removal of trehalose from the diet led to accumulation of Dilp3 but not Dilp2 (Fig. 2-6b). Starvation for amino acids had the opposite effect, increasing the intensity of Dilp2 staining, as reported, but not of Dilp3. The expression of Dilp2 and Dilp3 mRNA was unchanged in response to these dietary conditions (Fig. 2-6c). Finally, larvae raised on food containing trehalose had a higher level of circulating Dilp3 protein in the hemolymph (Fig. 2-6d), consistent with the low Dilp3 levels in the IPCs under these conditions. Thus, whereas the mRNA levels of both Dilp2 and 3 have been shown to increase in response to a high sugar diet and to correlate with glucose and trehalose hemolymph concentrations (Musselman et al., 2011), our data indicate that only Dilp3 is regulated by sugar at the level of secretion. Taken together, we conclude that secretion of Dilp2 and Dilp3 is independently regulated by amino acids and trehalose, respectively.

How might different nutrient cues promote selective secretion of distinct insulin-like peptides? Individual secretion granules containing Dilps can be visualized within the IPCs by high-powered confocal imaging. Analysis of brains double-labeled for Dilp2 and

Figure 2-5

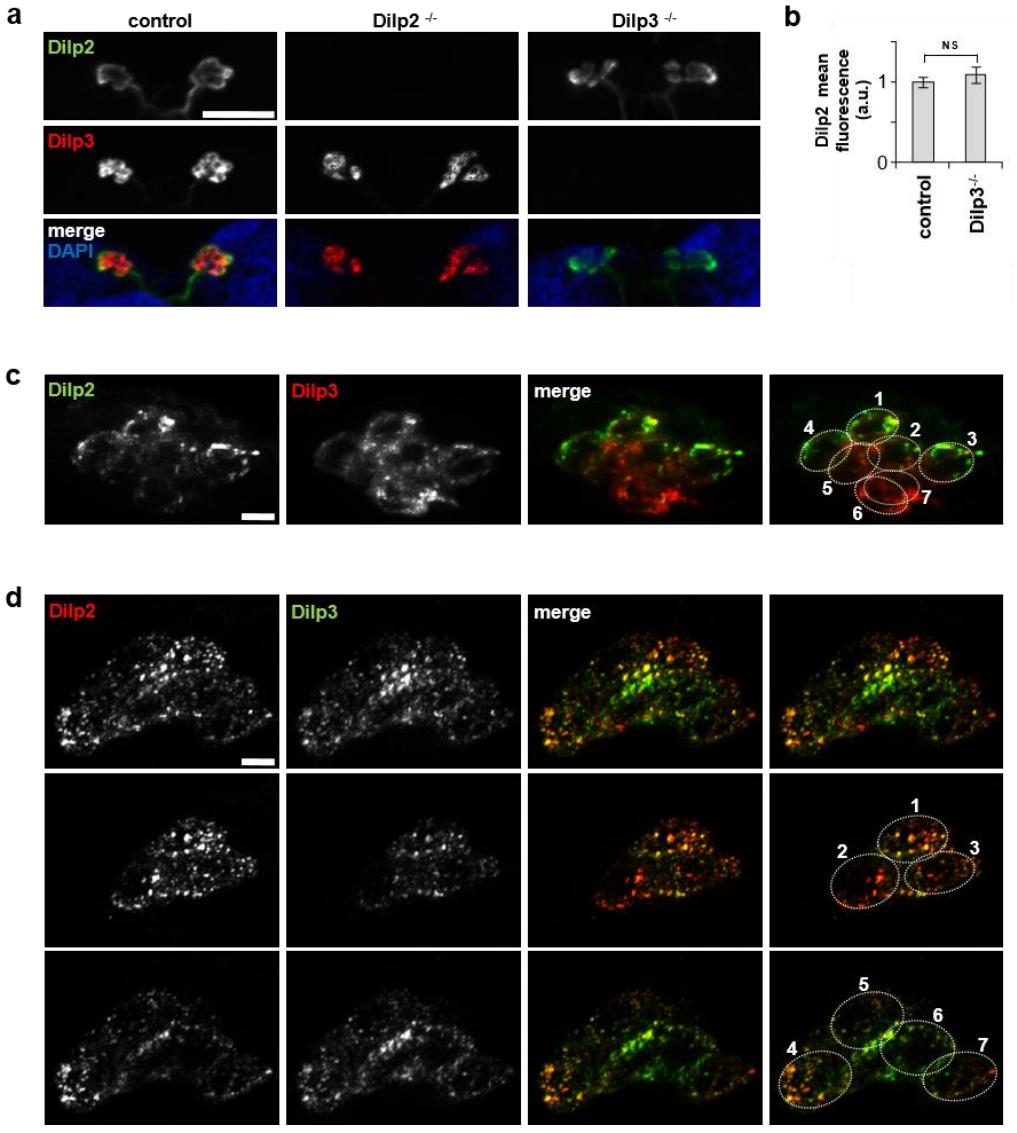
a
control
Dilp2 -/-
Dilp3 -/-
Dilp2
Dilp3
merge
DAPI
b
Dilp2 mean fluorescence (a.u.)
NS
1
0
control
Dilp3-/-
c
Dilp2
Dilp3
merge
1
2
3
4
5
6
7
d
Dilp2
Dilp3
merge
1
2
3
4
5
6
7

Figure 2-5: Antibody controls.

(a, b) Specificity of Dilp antibodies. Anti-Dilp2 labels the IPCs in control and *Dilp3*$^{-/-}$ but not *Dilp2*$^{-/-}$ larvae. Anti-Dilp3 labels the IPCs in control and *Dilp2*$^{-/-}$ but not *Dilp3*$^{-/-}$ larvae. Dilp2 fluorescence intensity is not significantly different between control and *Dilp3*$^{-/-}$ IPCs. Data represent mean±s.e.m., n=11. NS: P>0.05, student's t-test. **(c)** Additional confocal image showing distinct patterns of Dilp2 and Dilp3 localization in IPCs (rabbit anti-Dilp2, mouse anti-Dilp3 as in Figure 4) following 4 hr complete starvation. **(d)** Combined Z-stack (top) and individual (middle, bottom) confocal sections of Dilp2- and Dilp3-stained IPCs, using independently-derived 1° antibodies from those shown in Figures 4 and S2C (rat anti-Dilp2, Texas Red anti-rat; rabbit anti-Dilp3, FITC anti-rabbit). Scale bars 50 μm (a), 5 um (c, d). Images in c and d are each representative of two independent experiments, n=7.

Figure 2-6

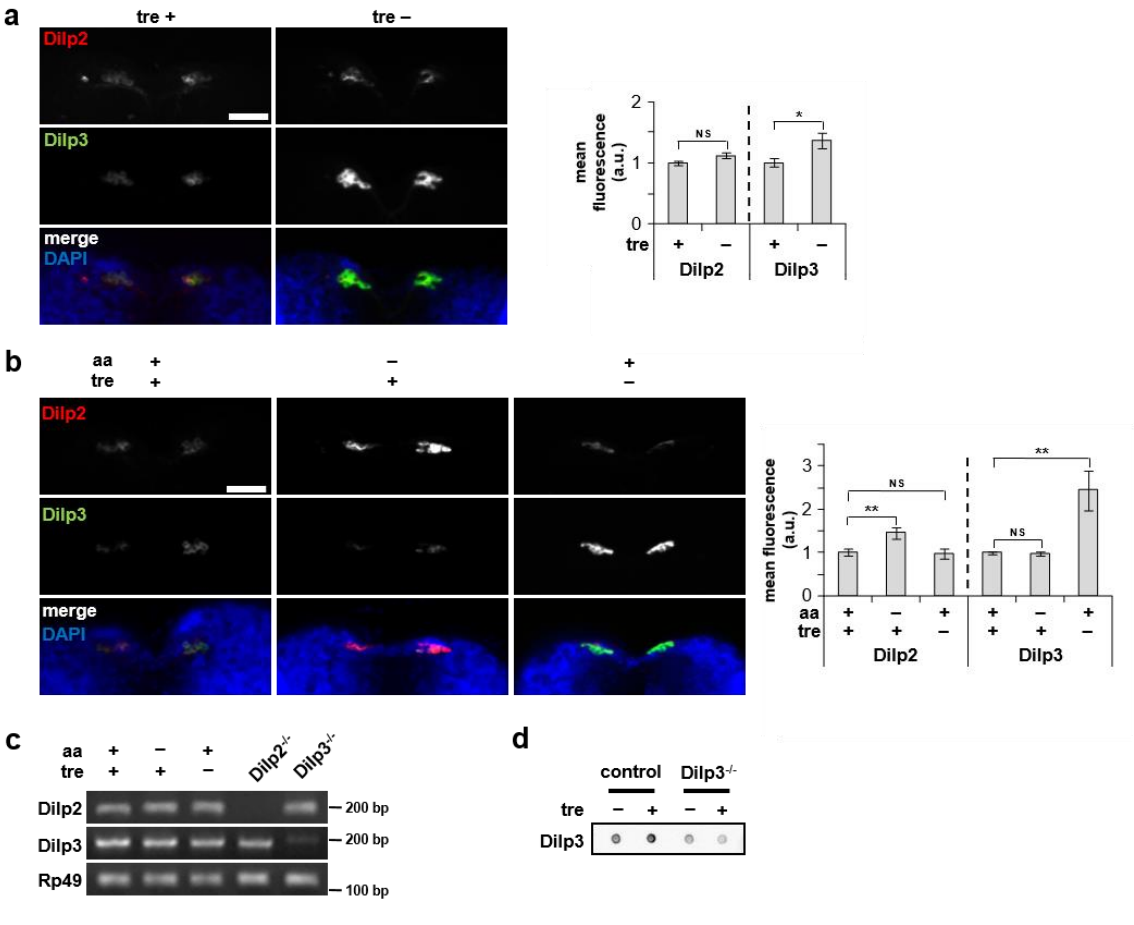
a
tre +
tre –
Dilp2
Dilp3
merge
DAPI
mean fluorescence (a.u.)
NS
*
tre
Dilp2
Dilp3
b
aa
tre
Dilp2
Dilp3
merge
DAPI
mean fluorescence (a.u.)
NS
**
Dilp2
Dilp3
c
aa
tre
Dilp2-/-
Dilp3-/-
Dilp2
Dilp3
Rp49
200 bp
200 bp
100 bp
d
control
Dilp3-/-
tre
Dilp3
e
Dilp2
Dilp3
merge
1
2
3
4
5
6
7

Figure 2-6: Trehalose promotes secretion of Dilp3.

(a) Confocal images showing Dilp2 and Dilp3 protein following *ex vivo* incubation in the presence or absence of trehalose. Incubation in media lacking trehalose leads to Dilp3 accumulation in the IPCs, whereas Dilp2 staining remains low under both conditions. **(b)** Accumulation of Dilp2 and Dilp3 in response to *in vivo* starvation for amino acids (aa) or trehalose. Levels of Dilp2 and Dilp3 are low in the IPCs of larvae raised on agar/tryptone/trehalose food. Dilp2 accumulates in response to lack of dietary amino acids (tryptone) but not trehalose, whereas Dilp3 accumulates in larvae raised on food lacking trehalose but not amino acids. Images in a and b are representative of eight larvae. Data were assessed by Student's *t*-test and are represented as mean±s.d. *$p<0.05$, **$p<0.01$, NS $p>0.05$.a.u., arbitrary units.**(c)** Levels of *Dilp2* and *Dilp3*mRNAin response to *in vivo* starvation for amino acids or trehalose, analyzed by semi-quantitative RT-PCR. *Rp49*serves as internal control. **(d)** Dot blot analysis of circulating Dilp3 levels in larvae grown on food with or without trehalose *in vivo*. Blot is representative of three independent experiments. **(e)** High-magnification combined Z-series stack of confocal sections of IPCs from 24 hr starved larvae, demonstrating distinct intracellular localization and biased expression of Dilp2 and Dilp3. Image is representative of three experiments, n = 7 larvae. Scale bars represent 50 µm in (a) and (b), and 5 µm in (e).

Dilp3 revealed that while some of these granules contain both Dilps, many contain largely either Dilp2 or Dilp3 (Fig. 2-5c,d, Fig. 2-6e). Interestingly, granules containing Dilp2 or Dilp3 tend to segregate to distinct regions of the cell. In addition, many individual IPCs show a clear bias in the levels of one Dilp over another. Thus, activation of distinct release pathways and/or subclasses of IPCs may contribute to these nutrient-selective responses.

An AKH-Dilp3 relay mediates trehalose-dependent TOR signaling

In mammals, ATP-sensitive potassium channels in the pancreatic beta cells play a critical role in sensing glucose levels and regulating insulin secretion. Interestingly, Drosophila homologs of these channel subunits are absent from larval IPCs, but instead are specifically expressed in the corpora cardiaca (CC) cells of the ring gland (Kim and Rulifson, 2004). These cells express the glucagon-like hormone AKH, and they make contact with processes from the IPCs. We found that RNAi-mediated depletion of AKH in the CC, or ablation of the CC itself, inhibited fat body TOR activation in response to trehalose (Fig. 2-7a; see Fig. 2-8a for depletion and ablation controls). Null mutation of the AKH receptor *AKHR* showed a similar block in TOR activation (Fig. 2-7b). Conversely, overexpression of AKH increased TOR activity in both the presence and absence of trehalose (Fig. 2-7c).

The influence of AKH signaling on trehalose-dependent TOR activation suggested that secretion of AKH may be regulated by trehalose. Although previous studies using fluorescent calcium sensors indicate that acute reduction in trehalose may stimulate secretion from CC cells (Kim and Rulifson, 2004), AKH protein levels in the

Figure 2-7

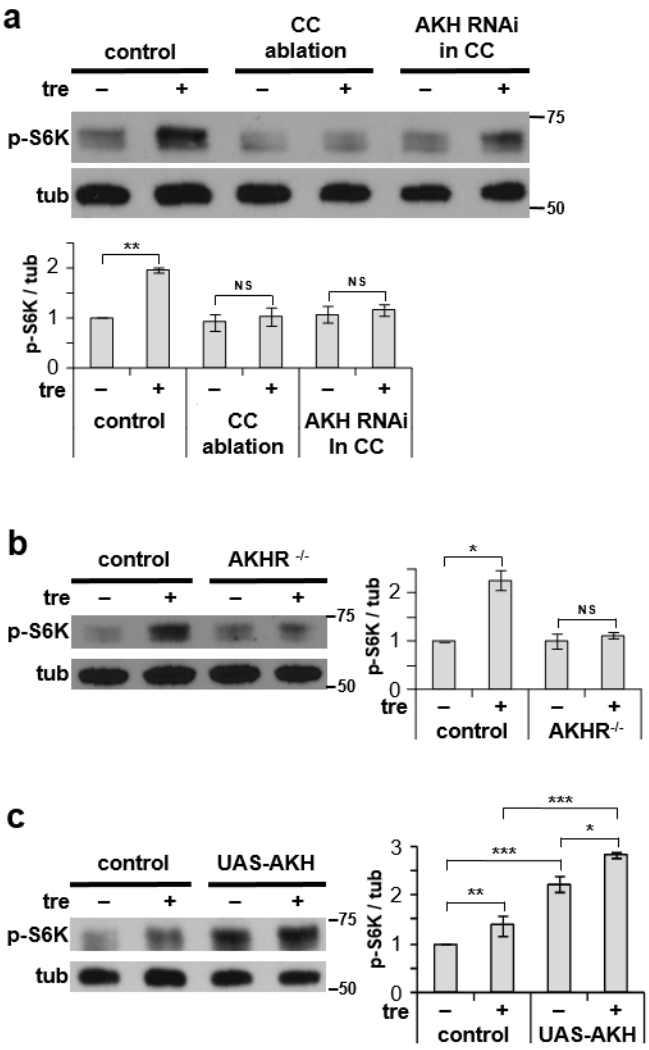
a
control
CC ablation
AKH RNAi in CC
tre
p-S6K
tub
75
50
p-S6K / tub
**
NS
NS
b
control
AKHR -/-
*
NS
AKHR-/-
c
control
UAS-AKH
***
*
**
UAS-AKH

Figure 2-7: Activation of TOR by trehaloserequires AKH signaling.

(a, b) Trehalose-mediated *ex vivo* activation of fb-TOR is disrupted by ablation of the CC *(AKH-GAL4 / UAS-reaper)* or depletion of *AKH* from the CC *(AKH-GAL4 / UAS-AKH^{RNAi})* and by null mutation of the AKH receptor *($AKHR^{1}/AKHR^{1}$)*. **(c)** Overexpression of AKH *(Cg-GAL4 / UAS-Akh)* increases fb-TOR signaling in the presence and absence of trehalose *ex vivo*. Data represent mean±s.e.m. of three (a, b) or four (c) independent experiments. *p<0.05, **p<0.01, ***p<0.001, NS p>0.05; Student's *t*-test.

Figure 2-8

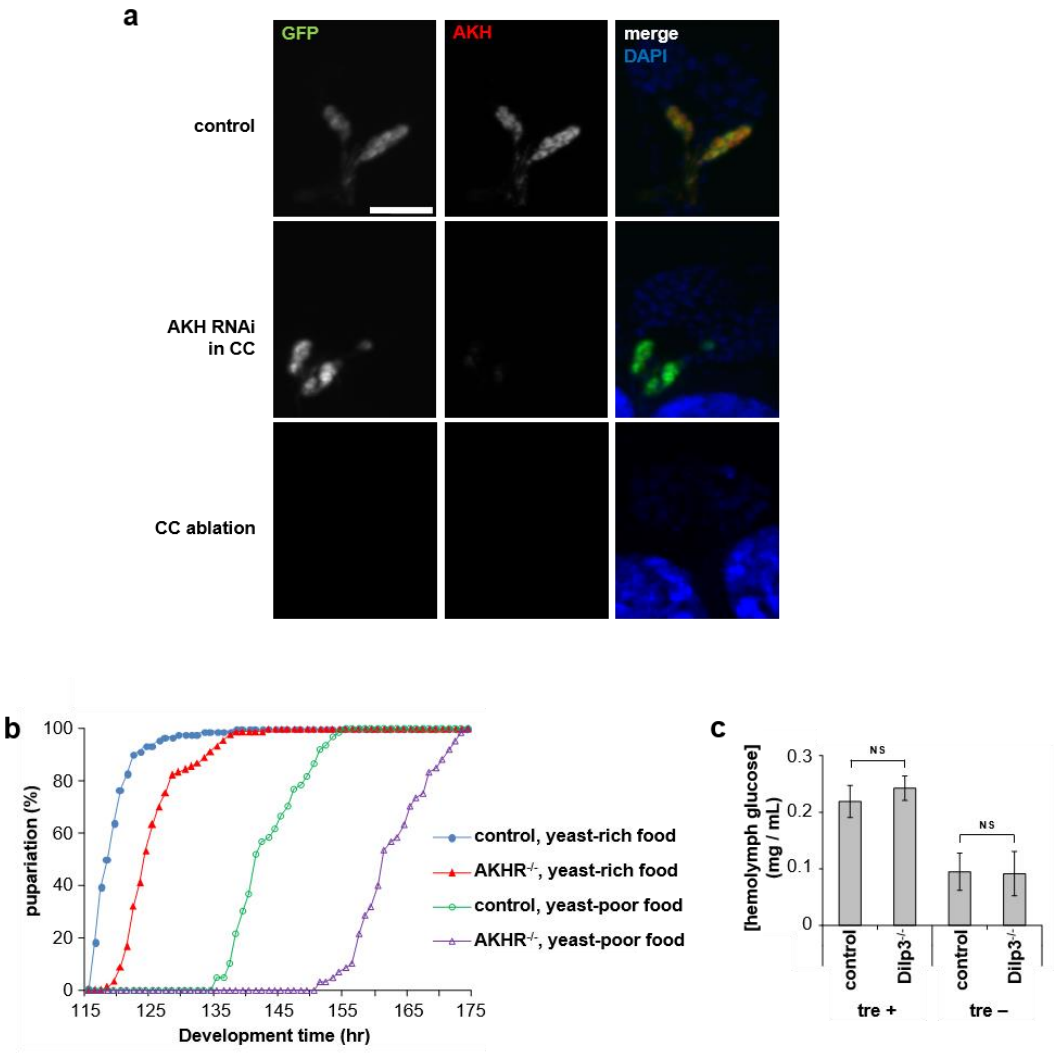
a
GFP
AKH
merge
DAPI
control
AKH RNAi
in CC
CC ablation
b
pupariation (%)
Development time (hr)
control, yeast-rich food
AKHR-/-, yeast-rich food
control, yeast-poor food
AKHR-/-, yeast-poor food
c
[hemolymph glucose]
(mg / mL)
NS
NS
control
Dilp3-/-
control
Dilp3-/-
tre +
tre –

Figure 2-8: AKH signaling controls and effects.

(a) Efficiency of AKH depletion and corpora cardiaca ablation. Anti-AKH staining reveals robust loss of AKH protein in CC cells expressing AKH dsRNA (middle; *AKH-GAL4 UAS-GFP / UAS-AKH^{RNAi})* and loss of the CC by targeted expression of reaper (bottom; *AKH-GAL4 UAS-GFP / UAS-reaper)*. Scale bar 50 µm. Representative images of seven larvae per genotype are shown. **(b)** Developmental timing measurements of *AKHR* null mutant and matched controls raised on rich and poor media (standard fly food with and without supplemental yeast, respectively). Data are from three vials of 30 larvae for each experimental condition. **(c)** Levels of circulating glucose in control and *Dilp3$^{-/-}$* larvae cultured in the presence or absence of trehalose *in vivo*. Data represent mean±s.e.m. of three independent experiments. NS: P>0.05, student's t-test.

CC were markedly increased following a 2-hr incubation in media lacking trehalose (Fig. 2-9a). This accumulation of AKH can be attributed to decreased secretion rather than increased production, as cycloheximide was included in these experiments to inhibit synthesis of new protein. Furthermore, CC-specific expression of the exocytosis inhibitor tetanus toxin, which has been shown to inhibit AKH secretion (Braco et al., 2012), prevented the reduction in AKH staining in response to trehalose (Fig. 2-9a). To confirm that release and diffusion of AKH is required for TOR activation in the fat body, we depleted AKH from the media by adding a blocking antibody against AKH, which led to a dose-dependent decrease in trehalose-stimulated fb-TOR activity (Fig. 2-9b). Altogether, these results indicate that secretion of AKH from the CC is an essential intermediary step in trehalose-responsive TOR activation.

The similar effects of AKH and Dilp3 are consistent with these factors acting in a common pathway to communicate trehalose levels to peripheral tissues. I therefore asked whether AKH signaling is required in the IPCs for fb-TOR activity. Indeed, IPC-specific knockdown of AKHR significantly inhibited activation of TOR in the fat body in response to trehalose (Fig. 2-10a). These results support the possibility that AKH signaling in the IPCs may be necessary for the trehalose-stimulated release of Dilp3. Consistent with this hypothesis, Dilp3 protein accumulated to high levels in the IPCs in response to depletion of AKH in the CC, in AKH receptor null mutants, and in response to depletion of AKHR specifically in the IPCs (Fig. 2-10b). These manipulations had no effect on Dilp3 mRNA levels (Fig. 2-10c). We conclude that the IPCs are important targets of AKH signaling, releasing Dilp3 in response to a trehalose-AKH relay from the CC cells.

Figure 2-9

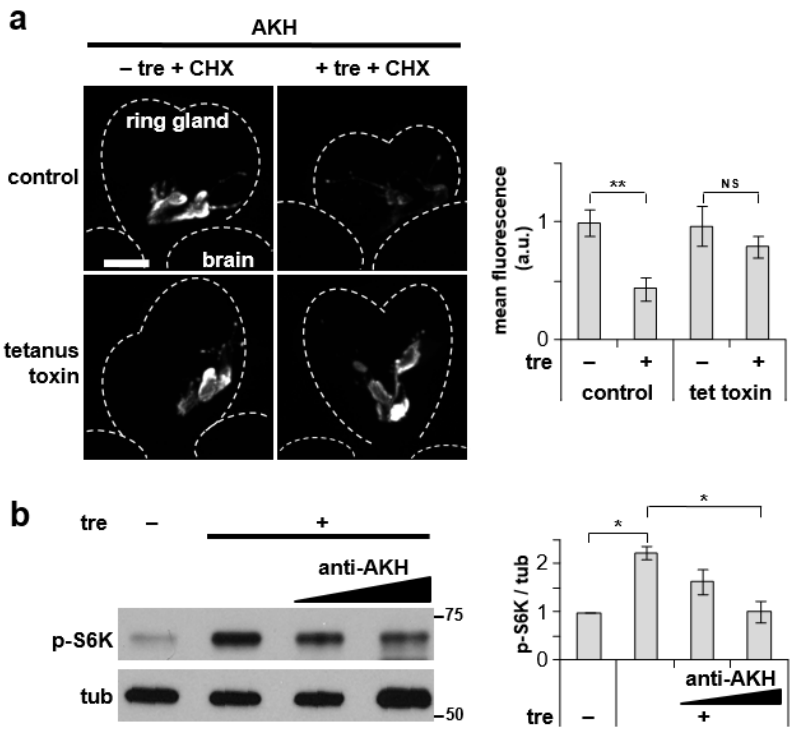
a
AKH
– tre + CHX
+ tre + CHX
ring gland
brain
control
tetanus toxin
mean fluorescence (a.u.)
**
NS
1
0
tre
–
+
–
+
control
tet toxin
b
tre
–
+
anti-AKH
p-S6K
tub
75
50
p-S6K / tub
*
*
2
1
0
anti-AKH
tre
–
+

Figure 2-9: Trehalose promotes AKH secretion to stimulate fb-TOR signaling.

(a) AKH antibody staining in the CC is reduced in response to trehalose during *ex vivo* incubation. CC-specific expression of tetanus toxin *(AKH-GAL4 / UAS-TeTxLC)* prevents the effect of trehalose. Cycloheximide (25 ug / ml) was included in all incubations to block AKH synthesis. Scale bar represents 50 µm. Representative images of seven ring glands per experimental condition are shown. **(b)** *Ex vivo* activation of fb-TOR signaling in response to trehalose is inhibited by blocking antibody against AKH ($5x10^{-2}$ and $2.5x10^{-2}$ serum dilution in M3 media). Blot is representative of three independent experiments. Bar graphs in a and b represent mean±s.e.m. *$p<0.05$, **$p<0.01$, NS $p>0.05$; Student's *t*-test.

Figure 2-10

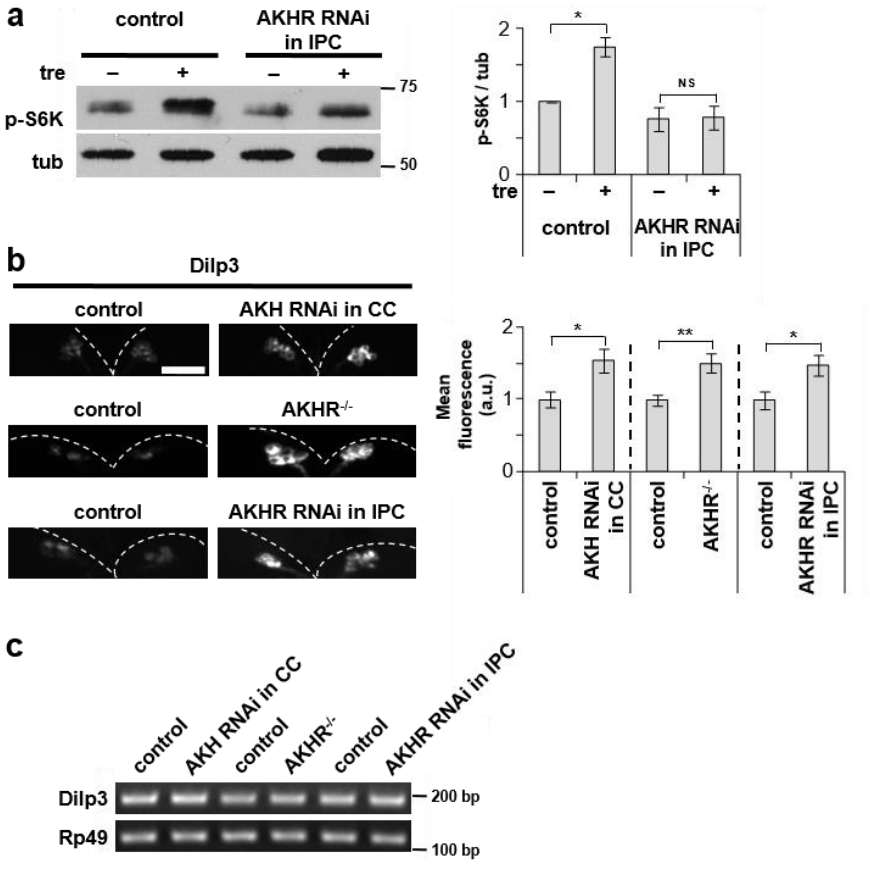
a
control
AKHR RNAi in IPC
tre
– + – +
p-S6K
tub
75
50
p-S6K / tub
2
1
0
*
NS
tre
– + – +
control
AKHR RNAi in IPC
b
DIlp3
control
AKH RNAi in CC
control
AKHR-/-
control
AKHR RNAi in IPC
Mean fluorescence (a.u.)
2
1
0
*
**
*
control
AKH RNAi in CC
control
AKHR-/-
control
AKHR RNAi in IPC
c
control
AKH RNAi in CC
control
AKHR-/-
control
AKHR RNAi in IPC
DIlp3
Rp49
200 bp
100 bp

Figure 2-10: AKH signaling in the IPCs is required for Dilp3 release.

(a) Depletion of *AKHR* by RNAi in the IPCs *(Dilp2-GAL4 / UAS-AKHR^{RNAi})* impairs TOR activation in the fat body in response to trehalose in the media. Blot is representative of three independent experiments. **(b)** Following *ex vivo* incubation in the presence of trehalose, Dilp3 protein accumulates in the IPCs in response to depletion of *AKH* in the CC *(AKH-GAL4 / UAS-AKH^{RNAi})*, null mutation of *AKHR (AKHR^{1}/Df (2L)Exel7027)*, and depletion of *AHKR* in the IPCs *(Dilp2-GAL4 / UAS-AKHR^{RNAi})*. Scale bar represents 50 µm. Representative images of eight animals per genotype are shown. Data in a and b were assessed by Student's *t*-test and are represented as mean±s.d. *p<0.05, **p<0.01, NS p>0.05. **(c)** Levels of *Dilp3* mRNA in the genotypes indicated in (b), analyzed by semi-quantitative RT-PCR. *Rp49* serves as internal control. Blot is representative of three independent experiments.

Dilp3 effects developmental rate and sugar homeostasis

Although insulin signaling is essential for normal growth and development, mutation of most individual Dilps has surprisingly little developmental effect, presumably due to redundancy and compensation between these factors (Gronke et al., 2010; Zhang et al., 2009). In particular, mutants lacking *Dilp3* develop with normal timing and show only a modest reduction in fecundity. We confirmed this lack of effect on developmental rate when *Dilp3* mutant and control animals were raised on rich media supplemented with yeast. However, growth on media lacking yeast resulted in a 30-hr delay in development in *Dilp3* mutant compared to control animals (Fig. 2-11a). These results reveal a cryptic growth requirement for Dilp3, presumably made evident here due to reduced levels of Dilp2 and/or Dilp5 under conditions of low amino acids. Interestingly, *AKHR* mutants showed a similarly enhanced developmental delay in the absence of dietary yeast (Fig. 2-8b), further supporting that AKH and Dilp3 function in a common pathway. In addition, levels of circulating trehalose were significantly higher in *Dilp3* mutant larvae than controls, particularly under the fed conditions required for Dilp3 release (Fig. 2-11b, Fig. 2-8c). Altogether, these results are consistent with a central role for Dilp3 in mediating growth and metabolism in response to dietary sugar.

Figure 2-11

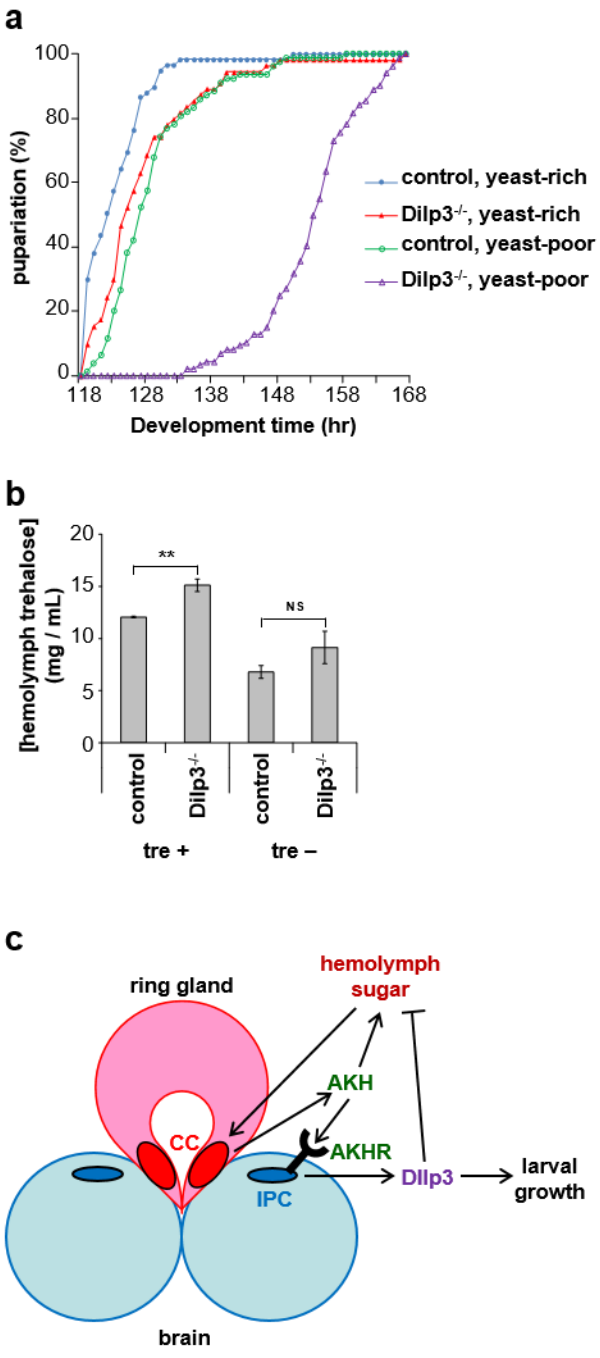
a
100
80
60
40
20
0
pupariation (%)
118
128
138
148
158
168
Development time (hr)
control, yeast-rich
Dilp3-/-, yeast-rich
control, yeast-poor
Dilp3-/-, yeast-poor
b
20
15
10
5
0
[hemolymph trehalose] (mg / mL)
**
NS
control
Dilp3-/-
control
Dilp3-/-
tre +
tre –
c
ring gland
hemolymph sugar
AKH
CC
AKHR
IPC
Dilp3
larval growth
brain

Figure 2-11: Dilp3 affects larval growth and sugar homeostasis.

(a) Developmental timing from egg laying to pupariation of control and *Dilp3*$^{-/-}$ mutants raised on rich and poor media (standard fly food with and without supplementary yeast, respectively). Data are from three vials of 30 larvae for each experimental condition. **(b)** Levels of circulating trehalose in control and *Dilp3*$^{-/-}$ larvae cultured in the presence or absence of trehalose *in vivo*. Data of three independent experiments were assessed by Student's *t*-test and are represented as mean±s.d. **p<0.01, NS p>0.05. **(c)**The results are consistent with a model whereby sugar stimulates release of AKH from the CC, which then triggers secretion of Dilp3 from the IPCs. Increased insulin signaling in peripheral tissues promotes larval growth, sugar uptake, and activation of TOR in the fat body, the latter of which may lead to further signal amplification through subsequent stimulation of Dilp2 release from the IPCs. The sugar-dependent secretion of AKH represents another potential positive feedback loop, which may be restricted by the counterbalancing effect of Dilp3. This model implies that in rapidly growing Drosophila larvae, co-regulation of AKH and insulin signaling may support high rates of insulin-dependent anabolic growth while preventing excessive storage of trehalose in the fat body, allowing other cells to use sugar to fuel cell growth.

CHAPTER 3: Mechanical stress regulates insulin signaling in an integrin-dependent manner

Mechanical stress is required for activation of fat body TOR *ex vivo*

As described in chapter 2 and published in Kim and Neufeld, 2015, *ex vivo* incubation of larval carcasses in M3 media with or without human insulin recapitulated the phosphor-S6K level in the fat body representing TOR activity under fed and starved conditions *in vivo*, respectively (Fig. 3-1a). Interestingly, the phosphorylation of S6K was also dependent on nutation (rocking/agitation) of the samples during incubation, which was performed in 1 ml of solution in a closed microfuge tube. Phosphorylation of 4EBP, another phosphorylation target of TOR, was also increased with nutation (Fig. 3-2a), further indicating that nutation promotes fb-TOR activation in the fat body *ex vivo*.

Why is nutation required for fb-TOR activity? I considered three possible factors that may be affected by nutation: mixing of the media, aeration of the media, and generation of mechanical stress. If uptake of insulin by fat body cells leads to a decrease in local insulin levels, mixing of the media may be required to maintain sufficient insulin concentrations for fb-TOR activation. To examine this possibility, I tested the rates at which fb-TOR activity decrease in response to lack of nutation. Fb-TOR activity was extinguished markedly in response to lack of nutation within 15 minutes (Fig. 3-1b). In addition, 10-fold higher concentration of insulin was unable to rescue fb-TOR activity in the absence of nutation (Fig. 3-2b), together suggesting that mixing and redistribution of ligands or nutrients is not a critical factor of fb-TOR activation.

To address a potential role for aeration, larval carcasses were incubated in the absence of air, by completely filling each tube with media. This led to a loss of fb-TOR activity (not shown), however the absence of a moving air bubble in these tubes also

Figure 3-1

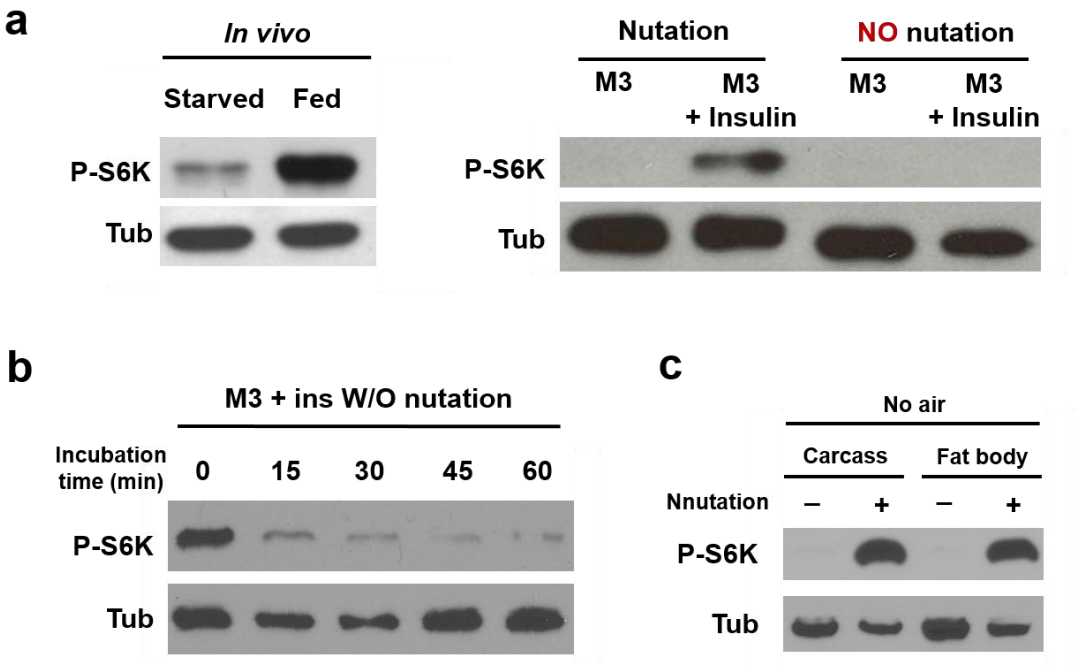
a
In vivo
Starved
Fed
P-S6K
Tub
Nutation
NO nutation
M3
M3 + Insulin
M3
M3 + Insulin
P-S6K
Tub
b
M3 + ins W/O nutation
Incubation time (min)
0
15
30
45
60
P-S6K
Tub
c
No air
Carcass
Fat body
Nnutation
–
+
–
+
P-S6K
Tub

Figure 3-1: Mechanical stress is required for activation of fat body TOR *ex vivo*

(a) Incubation *ex vivo* with nutation in the M3 media with or without 10 ug / ml of human insulin mimics fb-TOR activity under fed or starved conditions *in vivo*, respectively. TOR activity was measured by immunoblot of fat body lysates with p-S6K antibody. Without nutation, TOR activity is abolished even in the presence of human insulin *ex vivo*. Tubulin (tub) is a loading control.

(b) Fb-TOR activity was reduced within 15 min of incubation *ex vivo* without nutation in M3 + insulin media.

(c) Incubation of dissected carcass or fat body in M3 + insulin media without air bubble activates fb-TOR in a mechanical stress (M.S.)-dependent manner. A magnetic bar (7mm in length and 2mm in diameter) in the tube generated mechanical stress during nutation.

Figure 3-2


a
Nutation
+
–
P-S6K
P-4EBP
Tub
b
Ins
10 ug / mL
100 ug / mL
Nutation
+
–
+
–
P-S6K
Tub

Figure 3-2

(a) The levels of phosphorylated S6K and phosphorylated 4EBP were measured by immunoblot using p-S6K and p-4EBP antibodies, respectively, after *ex vivo* incubation in M3 media + insulin with or without nutation.

(b) 10-fold higher concentration of insulin (100 ug / ml) does not activate fb-TOR without nutation *ex vivo*.

greatly reduced the motion of carcasses in response to nutation. To counteract this effect, I placed a small mixing bar in each full tube, which restored the effect of nutation on carcass movement, and led to nutation-dependent activation of fb-TOR (Fig. 3-1c). This effect was observed on both whole larval carcasses and isolated fat body tissue. Together, these results suggest that neither mixing nor aeration can explain the effects of nutation on fb-TOR activation. Instead my data suggest that *ex vivo* nutation of the fat body causes some type of mechanical force, such as stretching or shear stress, and that this leads to activation of TOR in this tissue.

Body movement is necessary for activation of TOR in the fat body *in vivo*

Next, I investigated whether mechanical stress has a similar effect on TOR activity *in vivo*. To manipulate mechanical stress *in vivo*, crawling movement of mid-L3 larvae was restricted using two independent types of anesthesia: CO_2 gas and cold treatment at 4 ℃. Since crawling body movement is necessary for eating behavior, I performed experiments under complete starvation, which supplies water only, to exclude effects due to differences in food uptake. Each anesthetic treatment led to a reduction of TOR activity within 15 minutes, compared to non-anesthetized controls (Fig. 3-3a). After inhibition of body movement for 1 hr by CO_2 treatment, TOR activity was barely detectable (Fig. 3-4a), similar to the effects of incubation without mechanical stress *ex vivo*. Importantly, I observed that incubation at 4 ℃ had no effect on TOR activation by nutation *ex vivo* (Fig. 3-4b), suggesting that inhibition of body movement, not cold treatment itself, blocks TOR activity.

Figure 3-3

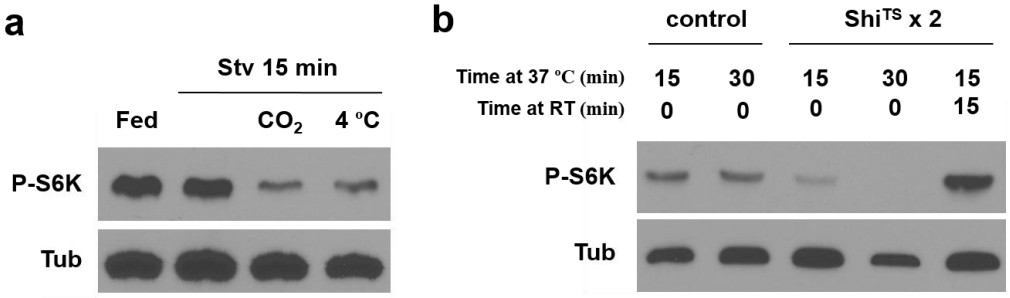
a
Stv 15 min
Fed
CO2
4 °C
P-S6K
Tub
b
control
Shi^TS x 2
Time at 37 °C (min)
Time at RT (min)
15
30
15
30
15
0
0
0
0
15
P-S6K
Tub

Figure 3-3: Body movement is necessary for activation of TOR in the fat body *in vivo*

(a) Inhibition of larval crawling body movement by continuous exposure to CO_2 gas or 4 ℃ cold treatment under starvation in agar + water for 15 min decreases TOR activity in fat body extracts compared to starvation only.

(b) Control and Ok6-Gal4 / Shi^{TS} x2 larvae were cultured at 37 ℃ or room temperature (RT) for designated time to inhibit larval crawling body movement. Inhibition of larval body movement causes a severe defect of TOR activation compared to control. This defective TOR activity is rescued by temperature shift from 37 ℃ to RT for 15 min, which allows larvae to crawl again.

Figure 3-4

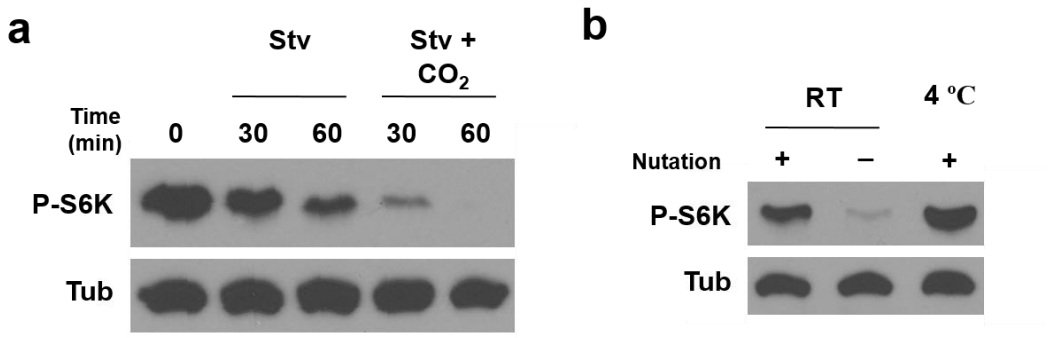
a
Stv
Stv +
CO_2
Time
(min)
0
30
60
30
60
P-S6K
Tub
b
RT
4 °C
Nutation
+
–
+
P-S6K
Tub

Figure 3-4

(a) Interruption of body movement by CO_2 for 1 hr abolishes TOR activity under starvation *in vivo*.

(b) Fb-TOR activity remains high at 4 ℃ during *ex vivo* incubation in M3 media + insulin with mechanical stress.

To test this idea further, I expressed a temperature-sensitive mutant allele of Shibire, which blocks vesicle recycling at the synapse, in the motor neurons to prevent crawling body movement, as has been described previously (Mehnert and Cantera, 2008). Shifting from permissive temperature (room temperature, RT) to restrictive temperature (37 ℃) paralyzed the larvae, and led to a loss of TOR activity within 30 min (Fig. 3-3b). This effect could be rapidly rescued by a shift from restrictive back to permissive temperature, which restored larval movement. My data strongly support the idea that mechanical stress caused by crawling body movement is required for activation of TOR *in vivo*.

Localization of insulin signaling components is regulated by mechanical stress

To address how mechanical stress affects TOR signaling, I examined the localization, activity and sufficiency of upstream signaling components in the presence and absence of nutation. First, the effect of mechanical stress on the distribution of the InR and two of its adapter proteins, Chico and Lnk (Almudi et al., 2013) was examined by visualizing fluorescently tagged version of these proteins by confocal microscopy. Each of these proteins showed a partial localization to the plasma membrane of fat body cells after 2 hours of *ex vivo* incubation with nutation (Fig. 3-5a). This membrane localization was most obvious for Lnk and weakest for InR. In contrast, after 2 hours without nutation, the membrane localization of each protein was reduced. Nutation had no appreciable effect on the overall levels of these proteins (Fig. 3-6).

As recruitment of insulin signaling components to the plasma membrane is important for their activation, I next examined the effects of nutation on markers of

Figure 3-5

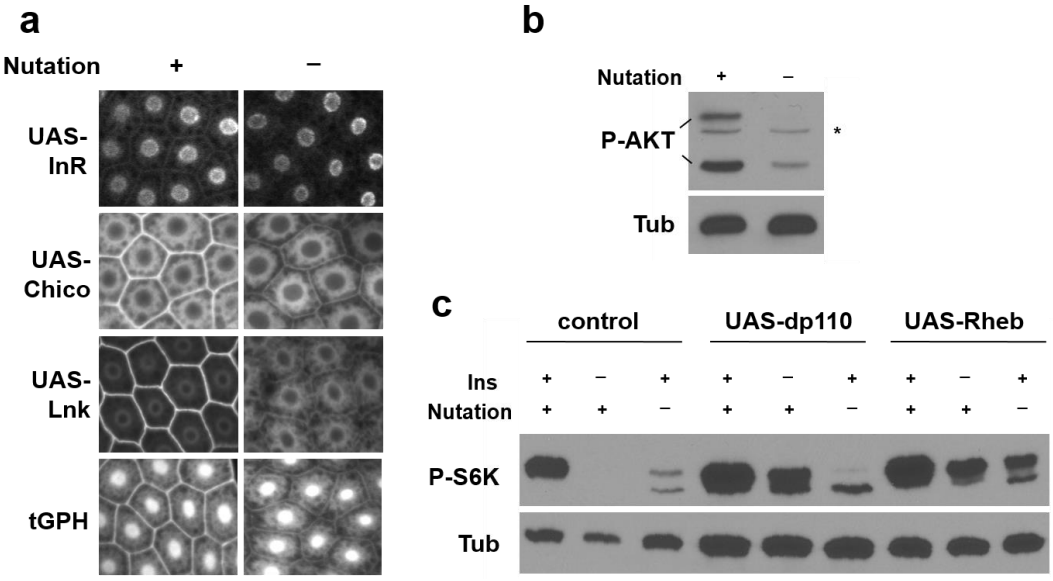
a
Nutation + –
UAS-InR
UAS-Chico
UAS-Lnk
tGPH
b
Nutation + –
P-AKT
*
Tub
c
control
UAS-dp110
UAS-Rheb
Ins
Nutation
P-S6K
Tub

Figure 3-5: Localization of insulin signaling components is regulated by mechanical stress

(a) Mechanical stress triggers localization of UAS-InR-CFP, UAS-Chico-RFP, and UAS-Lnk-RFP (each driven by Cg-Gal4) and of tubulin:GFP-PH domain (tGPH) to the membrane of fat body cells after 2 hr incubation in M3 + insulin media.

(b) The level of phosphorylated AKT, detected by immunoblot of fat body extracts, is elevated by mechanical stress *ex vivo*.

(c) loss of fb-TOR activity due to lack of insulin in the media, but not lack of mechanical stress, is partially rescued by fat body-specific overexpression of Dp110 using Cg-Gal4. Overexpression of Rheb in the fat body partially rescues fb-TOR activity in the absence of insulin or mechanical stress.

Figure 3-6

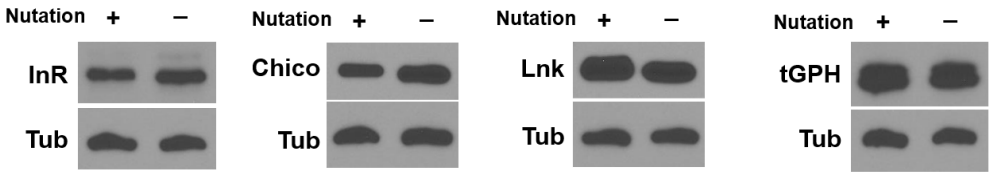
Nutation + –
InR
Tub
Nutation + –
Chico
Tub
Nutation + –
Lnk
Tub
Nutation + –
tGPH
Tub

Figure 3-6

The protein levels of InR, Chico, Lnk, and tGPH was measured by immunoblot after 2-hr *ex vivo* incubation in M3 + insulin media with or without mechanical stress.

insulin signaling activity. The tGPH marker consists of a GFP-tagged pleckstrin homology domain, which is recruited to the plasma membrane in response to increased levels of PIP3, and thereby serves as a measure of PI3K activity (Britton et al., 2002). Consistent with a positive effect of mechanical stress on insulin signaling, tGPH was also recruited to the membrane in response to nutation (Fig 3-5a). I also examined the status of AKT phosphorylation at Ser505, another well characterized marker of insulin/PI3K activity (Scanga et al., 2000). Phospho-AKT levels were high in fat body extracts from carcasses nutated *ex vivo*, and greatly reduced in samples without nutation (Fig 3-5b). Together, these data indicate that mechanical stress leads to activation of insulin signaling, at least in part through recruitment of proximal signaling components to the cell membrane.

From InR to TOR, major components in the insulin signaling pathway were affected by mechanical stress. To better understand at what point in the pathway this stress signal is integrated, epistatic analysis was performed. I overexpressed well-characterized activators of insulin signaling, Dp110, the catalytic subunit of PI3K, or Rheb, the direct activator of TOR and asked whether this was sufficient to rescue defective fb-TOR activity caused by the absence of mechanical stress or insulin in the media. Overexpression of Dp110 partially rescued TOR activity in the absence of insulin, but was unable to do so in the absence of mechanical stress (Fig. 3-5c). In contrast, overexpression of Rheb caused significant rescue in the absence of either insulin or mechanical stress. Together with the localization and activity data above, these results suggest that mechanical stress regulates insulin signaling at least two points: early in

pathway at the level of the InR/chico/Lnk complex, and farther downstream in between PI3K and Rheb.

Integrin signaling is required for mechanical stress-dependent insulin signaling

How are mechanical forces sensed and transmitted to the insulin pathway? Integrin-dependent signaling is one of the mechanisms transmitting mechanical stress in mammals (Tahimic et al., 2013). I therefore decided to examine the potential role of this pathway and the ECM in mediating the effects of mechanical stress on insulin signaling.

The Drosophila larval fat body expresses the collagen IV protein Viking (Vkg), which is a component of ECM (Pastor-Pareja and Xu, 2011). Consistent with its role as a substrate for cellular attachment, GFP-tagged Vkg (vkg-GFP) was localized close to the membrane and between fat body cells (Fig. 3-7a). Addition of collagenase in the M3 + insulin media *ex vivo* led to dissociation of fat body cells and loss of fb-TOR activity (Fig. 3-7b), which suggests that an intact ECM is necessary for fb-TOR activation.

Since ECM is a common ligand of integrin (Jean et al., 2011), I performed clonal RNAi screening of known integrins and downstream components, and found that depletion of integrin beta PS (not shown) or talin led to reduced tGPH localization at the membrane (Fig. 3-7c). This was accompanied by an altered morphology of these cells, which appeared to have reduced cell-cell contact. My data suggest that components of ECM-integrin signaling are required for mechanical stress-dependent TOR activation in the fat body.

Figure 3-7

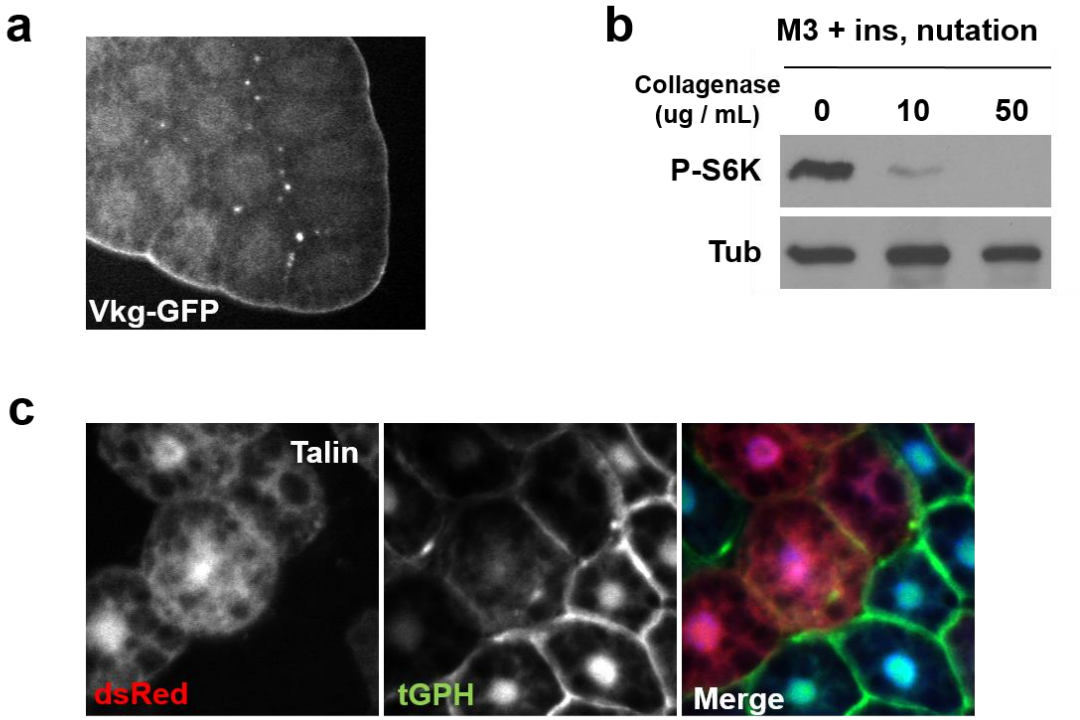
a
Vkg-GFP
b
M3 + ins, nutation
Collagenase
(ug / mL)
0
10
50
P-S6K
Tub
c
Talin
dsRed
tGPH
Merge

Figure 3-7: Integrin signaling is required for mechanical stress-dependent insulin signaling

(a) Viking-GFP is localized around the periphery of the larval fat body.

(b) Addition of collagenase in the M3 + insulin media ex vivo abolishes mechanical stress-dependent fb-TOR activity.

(c) Knock down of talin in dsRed-marked clones of the fat body leads to decreased localization of tGPH at the membrane.

CHAPTER 4: Discussion

Note to readers: A portion of this chapter was published in the journal *Nature Communications* 6:6846, 2015. In recognition that this work involved collaboration between the authors, this chapter uses the first person plural ("we") instead of first person singular ("I"). Individual contributions to this work are described in APPENDIX. Nature Publishing Group allows authors to reproduce articles for their thesis without permission. Refer to http://www.nature.com/reprints/permission-requests.html for more details.

The dual roles of insulin in promoting both cell growth and sugar homeostasis impose a unique challenge during periods of high growth such as larval and fetal development: sustained insulin signaling is required for normal developmental growth, yet circulating sugar concentrations must be maintained at a steady level under varying nutritional conditions. The results presented here suggest that in Drosophila larvae, this challenge is met in part through the coupled secretion of Dilp3 and AKH (Fig. 2-11c). This allows for normal hemolymph sugar concentrations despite relatively high Dilp levels, due to the counteracting effects of AKH. Although these hormones have opposing effects on hemolymph sugar concentrations akin to those of mammalian insulin and glucagon, their mechanisms of action are distinct. Ablation of the IPCs or deletion of Dilps 1-5 leads to increased hemolymph sugar concentrations (Rulifson et al., 2002; Zhang et al., 2009), likely reflecting a conserved role of Dilps in promoting glucose utilization and uptake through trafficking of glucose transporters (Crivat et al., 2013). In contrast, manipulation of AKH signaling, through CC ablation or AKH overexpression, strongly affects the concentration of trehalose, but has little or no effect on glucose levels (Lee and Park, 2004). This hypertrehalosemic effect of AKH is widely conserved in insects, and reflects the unique features of trehalose as both a circulating and storage form of carbohydrate. Due to the non-reactive, non-reducing properties of trehalose, its concentration can vary over a much wider range than glucose without causing cellular damage (Becker et al., 1996). Trehalose concentrations are commonly more than 10-fold higher than those of glucose, presumably due to the rapid conversion of glucose to trehalose in the fat body by trehalose-6-phosphate synthase (Chen and Haddad, 2004). This may counteract the low efficiency of insect open circulatory systems, bringing high

concentrations of trehalose directly to cells, each molecule of which can be cleaved within the cell to provide 2 glucose molecules as needed. Thus, the effect of AKH on trehalose and total sugar levels likely masks smaller changes in glucose concentrations that may be more directly regulated by Dilps. Finally, in contrast to their opposing effects on sugar homeostasis, it is notable that AKH and insulin signaling act in the same direction to promote expression of the α-glucosidase gene *target of brain insulin (tobi)* (Buch et al., 2008). Together with the stimulation of Dilp3 secretion by AKH described here, these findings indicate that in addition to its glucagon-like role, AKH may also function as a homolog to GLP-1, a positive regulator of mammalian insulin signaling (Drucker, 2006).

In contrast to the effect of trehalose as an autophagy suppressor described here, trehalose has been shown to activate autophagy in cultured mammalian cells, through undefined mechanisms (Sarkar et al., 2007). Recently, Inoue and coworkers demonstrated that sugars such as trehalose, sucrose and raffinose that cannot be hydrolyzed by mammalian cells induce autophagy, whereas cleavable disaccharides such as maltose and fructose do not (Higuchi et al., 2015). In this regard, it is notable that both the larval fat body and the CC cells express trehalase, which catalyzes conversion of trehalose to glucose (Kim and Rulifson, 2004). Indeed, it is unclear whether trehalose might be directly sensed and imported by the CC, or first converted to glucose through trehalases expressed on the cell surface (Becker et al., 1996).

The division of labor between Dilp2 and Dilp3 in responding to amino acids and sugars likely contributes to the ability of insulin signaling to balance growth and metabolic requirements, allowing overall insulin signaling to remain high in growing

larvae, while individual Dilps fluctuate in response to specific changes in nutrient conditions. This view implies that each of the eight Dilps may have evolved unique physiological functions in line with their specific mode of regulation. Whether different Dilps are functionally distinct remains poorly understood, but key differences between Dilp2 and Dilp3 may make them uniquely suited for growth and sugar homeostasis, respectively. For example, Dilp2 has been shown to have the strongest growth-promoting properties of Dilps1-7 when overexpressed during larval development (Ikeya et al., 2002). Notably, the insulin-binding factors Imp-L2 and dALS are able to form protein complexes with Dilp2 but not Dilp3, whereas Dilp3 but not Dilp2 interacts strongly with the insulin receptor decoy SDR (Arquier et al., 2008; Okamoto et al., 2013), suggesting that individual Dilps may engage the insulin receptor in qualitatively different ways. Interestingly, expression of Dilp5 is up-regulated in *dilp2* mutants and down-regulated in *dilp3* mutants (Gronke et al., 2010), indicating that these factors can have different and even opposing cellular effects, despite utilizing the same insulin receptor. Finally, recent studies have shown that selective outputs of insulin signaling can show distinct responses to transient vs. sustained patterns of receptor activation (Kubota et al., 2012). In this regard, we note that although we show here that Dilp3 but not Dilp2 is involved in acute responses to altered sugar levels, a chronic high sugar diet can increase the circulating levels of overexpressed Dilp2 (Musselman et al., 2011; Pasco and Leopold, 2012), and mutation of *dilp2* leads to increased hemolymph trehalose levels by adulthood (Gronke et al., 2010). As secretion of Dilp2 is promoted by activation of TOR in the fat body (Geminard et al., 2009), our finding that Dilp3 mediates fb-TOR activation by trehalose suggests that acute and chronic responses to sugar may be linked by a feed-forward

mechanism, whereby initial secretion of Dilp3 promotes subsequent Dilp2 secretion and further amplification of insulin signaling.

The selective secretion of Dilp2 and Dilp3 in response to distinct nutritional cues suggests that Dilp peptides contain unique sequence or structural cues targeting them to distinct secretory pathways, or that homophilic interactions promotes self-sorting of these peptides. Indeed, confocal analysis revealed clear segregation of Dilp2 and Dilp3 into different granules and intracellular regions. Selective secretion in response to a number of distinct stimuli has been described in eosinophils and mast cells: through a process known as piecemeal degranulation, specific cytokines are sequestered from secretion granules and shuttled to the plasma membrane in distinct secretory vesicles (Melo et al., 2013). This sequestration step involves direct ligand-receptor interaction within secretory pathway compartments. Similarly, release of specific classes of neurotransmitters from individual nerve terminals can be differentially stimulated in response to varying levels of Ca^{2+} concentration (Verhage et al., 1991). In mouse islet beta cells, glucagon-like peptide-1 was recently shown to selectively promote the secretion of newly synthesized secretory granules over that of granules previously docked at the plasma membrane (Xie et al., 2012). As the three receptors shown to regulate Dilp secretion – GABA-R (Rajan and Perrimon, 2012), adiponectinR (Kwak et al., 2013), and AKHR (present study)– are each members of the GPCR family, it will be interesting to investigate how different modes of downstream signaling ultimately affect selective Dilp release.

In chapter 3, I showed that mechanical stress is an essential regulator of insulin signaling. An interesting and relevant question is what the physiological roles of mechanical stress *in vivo* are. In the lifecycle of Drosophila, pupation is the only larval

stage that has no crawling movement. During this stage, there is no external source of nutrients, so the larval polyploid tissues induce a massive amount of developmental autophagy, which generates nutrients required for development of diploid tissues, such as the brain and imaginal discs, transforming to adult tissues after metamorphosis (Mulakkal et al., 2014). It is a common idea in the field that ecdysone, an insect hormone stimulating molting and pupation, has a role for inhibition of insulin signaling to induce developmental autophagy (Rusten et al., 2004). However, developmental autophagy is actively induced and causes autophagic apoptosis, whereas the peak of ecdysone occurs before metamorphosis and it is not maintained through metamorphosis (Denton et al., 2013; Thummel, 2001), suggesting that there might be additional mechanism regulating developmental autophagy.

It is possible that the effect of mechanical stress on insulin signaling in this stage plays a role in maintaining developmental autophagy. Lack of crawling movement may inhibit insulin signaling in the larval polyploid tissue, whereas growth and development of diploid tissues are protected by ALK signaling, which is independent of the level of insulin (Cheng et al., 2011). The decreased TOR activity in the polyploid tissues may induce developmental autophagy, which generates nutrients for diploid tissues. It will be interesting to investigate whether lack of mechanical stress in the larvae before pupation induces autophagy, which may be similar to developmental autophagy.

Lack of ECM, integrin beta PS, or talin caused defective insulin signaling even in the presence of insulin and mechanical stress, but the mechanism by which these players regulate insulin signaling is still unclear. One possibility is that integrin signaling regulates the responsiveness of InR to insulin. It has been reported that integrin

alphavbeta3 forms a cluster with IGF-1 and IGF-1R in mammalian ovary cells (Saegusa et al., 2009). Similarly, activated integrin beta PS by mechanical stress may form a cluster with insulin and InR. It has been shown that auto-inhibition of talin blocks activation of integrin beta PS and mutant form of talin, which is not capable to auto-inhibit, hyperactivates integrin signaling (Ellis et al., 2013). It is intriguing to test whether expression of this mutant talin is able to activate insulin signaling without mechanical stress.

Developing a model system using Drosophila to understand diabetes in humans is at the starting stage and there are lots of areas to improve. It has been shown that a high-sugar diet triggers insulin resistance in Drosophila (Musselman et al., 2011; Pasco and Leopold, 2012), but the mechanism is not yet understood. In my thesis work, I provided evidence that secretion of Dilp3 is regulated by dietary trehalose, which might help to explain the mechanism by which high-sugar diet leads to insulin resistance in this system. Moreover, my data show how mechanical stress can insulin sensitivity. This is reminiscent of the effect of exercise in T2D patients (Orozco et al., 2008). Finding of such similarities between Drosophila and mammals will accelerate developing Drosophila as a human disease model, suitable for screening to find therapeutic targets of diabetes in the near future.

CHAPTER 5: Methods

Note to readers: A portion of this chapter was published in the journal *Nature Communications* 6:6846, 2015. Nature Publishing Group allows authors to reproduce articles for their thesis without permission. Refer to http://www.nature.com/reprints/permission-requests.html for more details.

Drosophila strains

The following *D. melanogaster* strains were used: *AKHR[1]*, *AKHR[revA]* ((Gronke et al., 2007), gift of R. Kühnlein, Max Planck Institute, Göttingen, Germany); vkg-GFP ((Pastor-Pareja and Xu, 2011), gift of T. Xu, Yale University School of Medicine, New Haven, CT); tGPH ((Britton et al., 2002), gift of B.A. Edgar, Molecular and Cellular Biology program, Seattle, WA);*AKH[KK105063]* and *AKHR[KK109300]* RNAi lines (Vienna Drosophila RNAi Center, Vienna, Austria); UAS-InR-CFP, UAS-Chico-RFP, and UAS-Lnk-RFP ((Almudi et al., 2013), gift of H. Stocker, Institute of Molecular Systems Biology, Zürich, Switzerland); UAS-mChAtg8a (Chang and Neufeld, 2009); UAS-Rheb[EP50] (Scott et al., 2004); Akh-GAL4.L, Cg-GAL4.A, Df(2L)Exel7027, Dilp2-Gal4.R,*Dilp2[1]*, *Dilp3[1]*, *Dilp5[1]*, *Df(3L)Dilp1-4 Dilp5[4] Dilp7[1]*,Oregon-R-C, UAS-Akh.L, UAS-P110[wt], UAS-P110[D954A], UAS-rpr.C, UAS-TeTxLC.(-)Q, Ok6-Gal4, UAS-Shi^{TS}, and integrin beta PS and Talin RNAi lines were obtained from the Bloomington Drosophila Stock Center (Bloomington, IN).

Larval culture

Embryos were collected for 3-5 hours on standard fly food. For *in vivo* feeding experiments, early L3 larvae (85 - 90 hr after egg laying (AEL) @ 25 ℃) were transferred to agar/tryptone media containing 5.76 mg/ml of agar, 17 mg/ml of tryptone, 2 mg/ml of leucine with or without 26.6mg/ml of trehalose for 15-17 hr prior to dissection.

For *ex vivo* carcass incubation experiments, L3 larvae (72-77 hr AEL) were transferred to fresh standard fly food supplemented with granular yeast. After 24 hr,

seven larvae per condition were bisected and inverted, and digestive tracks removed. Dissected carcasses were incubated with nutation at room temperature in 1 mL of Shields and Sang M3 Insect Medium with or without trehalose (40 mg/mlor otherwise noted) for 2 hr (for western blotting) or 4 hr (autophagy experiments). M3 medium (S3652), trehalose (T0167), human insulin solution (I9278), Collagenase Type I (C0130), Earle's Balanced Salts Solution (E3024) and L-Leucine (L8000) were from Sigma-Aldrich (St. Louis MO).

Conditioned media was made by incubating brain and ring gland complexes from ten larvae for 2 hr in 1mL of M3 media containing 40 mg/ml trehalose. The recovered media was used immediately for incubation with carcasses from which the brain was removed.

Immunoblotting

Fat bodies from 5 larvae per sample were dissected in PBS and lysed directly in SDS sample buffer, with three or more biological replicates used for each experiment. Extracts were boiled 3 minutes, separated by polyacrylamide gel electrophoresis, and transferred to Immobilon-P membranes (Millipore, Billerica MA). Circulating Dilp3 levels were determined from hemolymph of 10 larvae per sample, diluted 1:100 in PBS and spotted (1 uL) onto methanol-soaked Immobilon-P membranes (Millipore, Billerica MA). Air-dried membranes were blocked in PBT + 5% BSA, and incubated overnight in blocking solution containing primary antibody. Signals were visualized using SuperSignalWest Pico chemiluminescent substrate (Thermo Scientific, Rockford, IL) with BioMax Light (Kodak, Rochester NY) or HyBlot CL autoradiography film (Denville Scientific,

Metuchen NJ), and quantitated using Adobe Photoshop software. Antibodies used were rabbit anti-phospho-T398 dS6K (1:250), rabbit anti-phospho-S505 dAkt (1:1,000), rabbit anti-dAkt(1:1,000), and rabbit anti-phospho-4EBP (1:500) (all from Cell Signaling Technology, Beverly MA), rabbit anti-Dilp3(1:1,000;gift of J. Veenstra, Université Bordeaux, Talence, France, (Veenstra et al., 2008)), rabbit anti-GFP (1:30,000) (A6455, Molecular Probes, Eugene OR), rabbit anti-dsRed (1:10,000) (#632496, Clontech Laboratories, Mountain View CA) and mouse anti-beta-tubulin E7 (1:1,000;Developmental Studies Hybridoma Bank, Iowa City IA).

Confocal imaging

Samples were prepared for confocal imaging as follows. 7-10 larvae were bisected and inverted in PBS, fixed 20 min in 4% paraformaldehyde / PBS, washed extensively in PBS + Triton X-100 (PBT; 0.3% or 0.1% for imaging IPCs or CCs, respectively), blocked in PBT + 5% bovine serum albumin (BSA), and incubated overnight in blocking solution containing primary antibody. After four washes in PBT, samples were incubated 2hr in blocking solution containing secondary antibody and washed four times. Carcasses after incubation *ex vivo* were directly used for fixation. For autophagy detection, samples were prepared, fixed, and washed as described above. Fixed tissues were dissected in PBS, mounted in Vectashield (Vector Labs, Burlingame, CA), and confocal images were collected on a Zeiss LSM710 confocal microscope and processed with Adobe Photoshop. The following antibodies were used for imaging experiments: rabbit anti-AKH (1:500), rabbit anti-Dilp2 (1:500), rabbit anti-Dilp3 (1:500), mouse anti-Dilp3 (1:500; all gifts of J. Veenstra, Université Bordeaux, Talence, France, (Veenstra et al., 2008)), rat anti-Dilp2

(1:500;gift of P. Leopold, Université de Nice, Nice,France, (Geminard et al., 2009)), rabbit anti-AKH (1:500; gift of J. Park, University of Tennessee, Knoxville, TN, (Lee and Park, 2004)).

Sugar measurement

Hemolymph sugar concentrations were determined as described previously (Tennessen et al., 2014). Briefly, 1 uL of hemolymph was obtained from 9-10 L3 larvae and mixed with 9 uL of trehalase buffer (5 mMTris pH 6.6, 137mM NaCl, 2.7 mMKCl). After incubation for 5 min at 95 ℃ and centrifugation for 10minat 4 ℃ at 15,000 rpm, the supernatant was used for sugar measurement. Glucose (GO) Assay Kit (GAGO-20, Sigma-Aldrich, St. Louis MO) was used according to manufacturer's instructions to measure glucose. For trehalose measurements, supernatants were first incubated at 37 ℃ overnight with trehalase (T8778-1UN, Sigma-Aldrich Co. St. Louis, MO), and glucose levels were then measured as above. Samples were read in 96-well plates (3641, Corning Life Sciences, Corning NY) at 540 nm using a Victor 3V 1420 multi label counter (Perkin Elmer, Waltham MA).

mRNA measurement

25 brains per sample were dissected in PBS, and total RNA was isolated using a Direct-zol RNA MiniPrepkit (R2050, Zymo Research, Irvine CA). RevertAid First Strand cDNA Synthesis Kit (K1621, Thermo Scientific, Pittsburgh PA) was used for reverse transcription of 600 ng of total RNA. Products were amplified by PCR using Ex Taq DNA Polymerase (RR001, Clontech Laboratories, Mountain View CA) for 34reaction

cycles, which was determined in control experiments to be within a linear range of amplification. Primer sequences were as follows: Dilp2-F 5'-CTGAGTATGGTGTGCGAGGA-3'; Dilp2-R 5'-CAGCCAGGGAATTGAGTACAC-3'; Dilp3-F 5'-GACCAAGAGAACTTTGGACCC-3'; Dilp3-R 5'-CAGCACAATATCTCAGCACCTC-3'; Rp49-F 5'-CGGATCGATATGCTAAGCTGT-3'; Rp49-R 5'-GCGCTTGTTCGATCCGTA-3'.

REFERENCES

Ahren, B. (2015). Glucagon--Early breakthroughs and recent discoveries. Peptides *67*, 74-81.

Almudi, I., Poernbacher, I., Hafen, E., and Stocker, H. (2013). The Lnk/SH2B adaptor provides a fail-safe mechanism to establish the Insulin receptor-Chico interaction. Cell communication and signaling : CCS *11*, 26.

Arquier, N., Geminard, C., Bourouis, M., Jarretou, G., Honegger, B., Paix, A., and Leopold, P. (2008). Drosophila ALS regulates growth and metabolism through functional interaction with insulin-like peptides. Cell metabolism *7*, 333-338.

Azim, H., Azim, H.A., Jr., and Escudier, B. (2010). Targeting mTOR in cancer: renal cell is just a beginning. Targeted oncology *5*, 269-280.

Baggio, L.L., and Drucker, D.J. (2007). Biology of incretins: GLP-1 and GIP. Gastroenterology *132*, 2131-2157.

Bathi, R.J., Parveen, S., Mutalik, S., and Rao, R. (2010). Rabson-Mendenhall syndrome: two case reports and a brief review of the literature. Odontology / the Society of the Nippon Dental University *98*, 89-96.

Beauchamp, E.M., and Platanias, L.C. (2013). The evolution of the TOR pathway and its role in cancer. Oncogene *32*, 3923-3932.

Becker, A., Schloder, P., Steele, J.E., and Wegener, G. (1996). The regulation of trehalose metabolism in insects. Experientia *52*, 433-439.

Braco, J.T., Gillespie, E.L., Alberto, G.E., Brenman, J.E., and Johnson, E.C. (2012). Energy-dependent modulation of glucagon-like signaling in Drosophila via the AMP-activated protein kinase. Genetics *192*, 457-466.

Britton, J.S., Lockwood, W.K., Li, L., Cohen, S.M., and Edgar, B.A. (2002). Drosophila's insulin/PI3-kinase pathway coordinates cellular metabolism with nutritional conditions. Developmental cell *2*, 239-249.

Buch, S., Melcher, C., Bauer, M., Katzenberger, J., and Pankratz, M.J. (2008). Opposing effects of dietary protein and sugar regulate a transcriptional target of Drosophila insulin-like peptide signaling. Cell metabolism *7*, 321-332.

Chang, Y.Y., and Neufeld, T.P. (2009). An Atg1/Atg13 complex with multiple roles in TOR-mediated autophagy regulation. Molecular biology of the cell *20*, 2004-2014.

Chang, Y.Y., and Neufeld, T.P. (2010). Autophagy takes flight in Drosophila. FEBS letters *584*, 1342-1349.

Chen, Q., and Haddad, G.G. (2004). Role of trehalose phosphate synthase and trehalose during hypoxia: from flies to mammals. The Journal of experimental biology *207*, 3125-3129.

Cheng, L.Y., Bailey, A.P., Leevers, S.J., Ragan, T.J., Driscoll, P.C., and Gould, A.P. (2011). Anaplastic lymphoma kinase spares organ growth during nutrient restriction in Drosophila. Cell *146*, 435-447.

Ciechanover, A., and Kwon, Y.T. (2015). Degradation of misfolded proteins in neurodegenerative diseases: therapeutic targets and strategies. Experimental & molecular medicine *47*, e147.

Cnop, M., Welsh, N., Jonas, J.C., Jorns, A., Lenzen, S., and Eizirik, D.L. (2005). Mechanisms of pancreatic beta-cell death in type 1 and type 2 diabetes: many differences, few similarities. Diabetes *54 Suppl 2*, S97-107.

Colombani, J., Andersen, D.S., and Leopold, P. (2012). Secreted peptide Dilp8 coordinates Drosophila tissue growth with developmental timing. Science *336*, 582-585.

Crivat, G., Lizunov, V.A., Li, C.R., Stenkula, K.G., Zimmerberg, J., Cushman, S.W., and Pick, L. (2013). Insulin stimulates translocation of human GLUT4 to the membrane in fat bodies of transgenic Drosophila melanogaster. PloS one *8*, e77953.

Denton, D., Aung-Htut, M.T., and Kumar, S. (2013). Developmentally programmed cell death in Drosophila. Biochimica et biophysica acta *1833*, 3499-3506.

DiMario, F.J., Jr., Sahin, M., and Ebrahimi-Fakhari, D. (2015). Tuberous Sclerosis Complex. Pediatric clinics of North America *62*, 633-648.

Drucker, D.J. (2006). The biology of incretin hormones. Cell metabolism *3*, 153-165.
Egger, G., and Dixon, J. (2014). Beyond obesity and lifestyle: a review of 21st century chronic disease determinants. BioMed research international *2014*, 731685.

Ellis, S.J., Goult, B.T., Fairchild, M.J., Harris, N.J., Long, J., Lobo, P., Czerniecki, S., Van Petegem, F., Schock, F., Peifer, M., *et al.* (2013). Talin autoinhibition is required for morphogenesis. Current biology : CB *23*, 1825-1833.

Feitelson, M.A., Arzumanyan, A., Kulathinal, R.J., Blain, S.W., Holcombe, R.F., Mahajna, J., Marino, M., Martinez-Chantar, M.L., Nawroth, R., Sanchez-Garcia, I., *et al.* (2015). Sustained proliferation in cancer: Mechanisms and novel therapeutic targets. Seminars in cancer biology.

Geminard, C., Rulifson, E.J., and Leopold, P. (2009). Remote control of insulin secretion by fat cells in Drosophila. Cell metabolism *10*, 199-207.

Gong, J., Robbins, L.A., Lugea, A., Waldron, R.T., Jeon, C.Y., and Pandol, S.J. (2014). Diabetes, pancreatic cancer, and metformin therapy. Frontiers in physiology *5*, 426.

Gronke, S., Clarke, D.F., Broughton, S., Andrews, T.D., and Partridge, L. (2010). Molecular evolution and functional characterization of Drosophila insulin-like peptides. PLoS genetics *6*, e1000857.

Gronke, S., Muller, G., Hirsch, J., Fellert, S., Andreou, A., Haase, T., Jackle, H., and Kuhnlein, R.P. (2007). Dual lipolytic control of body fat storage and mobilization in Drosophila. PLoS biology *5*, e137.

Hajiaghaalipour, F., Khalilpourfarshbafi, M., and Arya, A. (2015). Modulation of glucose transporter protein by dietary flavonoids in type 2 diabetes mellitus. International journal of biological sciences *11*, 508-524.

Harburger, D.S., and Calderwood, D.A. (2009). Integrin signalling at a glance. Journal of cell science *122*, 159-163.

Heppner, K.M., and Perez-Tilve, D. (2015). GLP-1 based therapeutics: simultaneously combating T2DM and obesity. Frontiers in neuroscience *9*, 92.

Higuchi, T., Nishikawa, J., and Inoue, H. (2015). Sucrose induces vesicle accumulation and autophagy. Journal of cellular biochemistry *116*, 609-617.

Ikeya, T., Galic, M., Belawat, P., Nairz, K., and Hafen, E. (2002). Nutrient-dependent expression of insulin-like peptides from neuroendocrine cells in the CNS contributes to growth regulation in Drosophila. Current biology : CB *12*, 1293-1300.

Jean, C., Gravelle, P., Fournie, J.J., and Laurent, G. (2011). Influence of stress on extracellular matrix and integrin biology. Oncogene *30*, 2697-2706.

Jewell, J.L., Russell, R.C., and Guan, K.L. (2013). Amino acid signalling upstream of mTOR. Nature reviews Molecular cell biology *14*, 133-139.

Johnson, S.C., Rabinovitch, P.S., and Kaeberlein, M. (2013). mTOR is a key modulator of ageing and age-related disease. Nature *493*, 338-345.

Kim, J., and Neufeld, T.P. (2015). Dietary sugar promotes systemic TOR activation in Drosophila through AKH-dependent selective secretion of Dilp3. Nature communications *6*, 6846.

Kim, S.K., and Rulifson, E.J. (2004). Conserved mechanisms of glucose sensing and regulation by Drosophila corpora cardiaca cells. Nature *431*, 316-320.

Kubota, H., Noguchi, R., Toyoshima, Y., Ozaki, Y., Uda, S., Watanabe, K., Ogawa, W., and Kuroda, S. (2012). Temporal coding of insulin action through multiplexing of the AKT pathway. Molecular cell *46*, 820-832.

Kwak, S.J., Hong, S.H., Bajracharya, R., Yang, S.Y., Lee, K.S., and Yu, K. (2013). Drosophila adiponectin receptor in insulin producing cells regulates glucose and lipid metabolism by controlling insulin secretion. PloS one *8*, e68641.

Lee, G., and Park, J.H. (2004). Hemolymph sugar homeostasis and starvation-induced hyperactivity affected by genetic manipulations of the adipokinetic hormone-encoding gene in Drosophila melanogaster. Genetics *167*, 311-323.

Long, R.K., Nishida, S., Kubota, T., Wang, Y., Sakata, T., Elalieh, H.Z., Halloran, B.P., and Bikle, D.D. (2011). Skeletal unloading-induced insulin-like growth factor 1 (IGF-1) nonresponsiveness is not shared by platelet-derived growth factor: the selective role of integrins in IGF-1 signaling. Journal of bone and mineral research : the official journal of the American Society for Bone and Mineral Research *26*, 2948-2958.

Lowell, C.A., and Mayadas, T.N. (2012). Overview: studying integrins in vivo. Methods in molecular biology *757*, 369-397.

Matteucci, E., Giampietro, O., Covolan, V., Giustarini, D., Fanti, P., and Rossi, R. (2015). Insulin administration: present strategies and future directions for a noninvasive (possibly more physiological) delivery. Drug design, development and therapy *9*, 3109-3118.

Mehnert, K.I., and Cantera, R. (2008). A peripheral pacemaker drives the circadian rhythm of synaptic boutons in Drosophila independently of synaptic activity. Cell and tissue research *334*, 103-109.

Melo, R.C., Liu, L., Xenakis, J.J., and Spencer, L.A. (2013). Eosinophil-derived cytokines in health and disease: unraveling novel mechanisms of selective secretion. Allergy *68*, 274-284.

Moon, J.S., and Won, K.C. (2015). Pancreatic alpha-Cell Dysfunction in Type 2 Diabetes: Old Kids on the Block. Diabetes & metabolism journal *39*, 1-9.

Mulakkal, N.C., Nagy, P., Takats, S., Tusco, R., Juhasz, G., and Nezis, I.P. (2014). Autophagy in Drosophila: from historical studies to current knowledge. BioMed research international *2014*, 273473.

Musselman, L.P., Fink, J.L., Narzinski, K., Ramachandran, P.V., Hathiramani, S.S., Cagan, R.L., and Baranski, T.J. (2011). A high-sugar diet produces obesity and insulin resistance in wild-type Drosophila. Disease models & mechanisms *4*, 842-849.

Musso, C., Cochran, E., Moran, S.A., Skarulis, M.C., Oral, E.A., Taylor, S., and Gorden, P. (2004). Clinical course of genetic diseases of the insulin receptor (type A and Rabson-Mendenhall syndromes): a 30-year prospective. Medicine *83*, 209-222.
Okamoto, N., Nakamori, R., Murai, T., Yamauchi, Y., Masuda, A., and Nishimura, T. (2013). A secreted decoy of InR antagonizes insulin/IGF signaling to restrict body growth in Drosophila. Genes & development *27*, 87-97.

Orozco, L.J., Buchleitner, A.M., Gimenez-Perez, G., Roque, I.F.M., Richter, B., and Mauricio, D. (2008). Exercise or exercise and diet for preventing type 2 diabetes mellitus. The Cochrane database of systematic reviews, CD003054.

Pandey, U.B., and Nichols, C.D. (2011). Human disease models in Drosophila melanogaster and the role of the fly in therapeutic drug discovery. Pharmacological reviews *63*, 411-436.

Pasco, M.Y., and Leopold, P. (2012). High sugar-induced insulin resistance in Drosophila relies on the lipocalin Neural Lazarillo. PloS one *7*, e36583.

Pastor-Pareja, J.C., and Xu, T. (2011). Shaping cells and organs in Drosophila by opposing roles of fat body-secreted Collagen IV and perlecan. Developmental cell *21*, 245-256.

Rajan, A., and Perrimon, N. (2012). Drosophila cytokine unpaired 2 regulates physiological homeostasis by remotely controlling insulin secretion. Cell *151*, 123-137.

Rorsman, P., and Braun, M. (2013). Regulation of insulin secretion in human pancreatic islets. Annual review of physiology *75*, 155-179.

Rulifson, E.J., Kim, S.K., and Nusse, R. (2002). Ablation of insulin-producing neurons in flies: growth and diabetic phenotypes. Science *296*, 1118-1120.

Rusten, T.E., Lindmo, K., Juhasz, G., Sass, M., Seglen, P.O., Brech, A., and Stenmark, H. (2004). Programmed autophagy in the Drosophila fat body is induced by ecdysone through regulation of the PI3K pathway. Developmental cell *7*, 179-192.

Saegusa, J., Yamaji, S., Ieguchi, K., Wu, C.Y., Lam, K.S., Liu, F.T., Takada, Y.K., and Takada, Y. (2009). The direct binding of insulin-like growth factor-1 (IGF-1) to integrin alphavbeta3 is involved in IGF-1 signaling. The Journal of biological chemistry *284*, 24106-24114.

Sarkar, S., Davies, J.E., Huang, Z., Tunnacliffe, A., and Rubinsztein, D.C. (2007). Trehalose, a novel mTOR-independent autophagy enhancer, accelerates the clearance of mutant huntingtin and alpha-synuclein. The Journal of biological chemistry *282*, 5641-5652.

Scanga, S.E., Ruel, L., Binari, R.C., Snow, B., Stambolic, V., Bouchard, D., Peters, M., Calvieri, B., Mak, T.W., Woodgett, J.R., *et al.* (2000). The conserved PI3'K/PTEN/Akt signaling pathway regulates both cell size and survival in Drosophila. Oncogene *19*, 3971-3977.

Schneider, D. (2000). Using Drosophila as a model insect. Nature reviews Genetics *1*, 218-226.

Scott, R.C., Schuldiner, O., and Neufeld, T.P. (2004). Role and regulation of starvation-induced autophagy in the Drosophila fat body. Developmental cell *7*, 167-178.

Simmons, K.M., and Michels, A.W. (2015). Type 1 diabetes: A predictable disease. World journal of diabetes *6*, 380-390.

Tahimic, C.G., Wang, Y., and Bikle, D.D. (2013). Anabolic effects of IGF-1 signaling on the skeleton. Frontiers in endocrinology *4*, 6.

Teleman, A.A., Ratzenbock, I., and Oldham, S. (2012). Drosophila: a model for understanding obesity and diabetic complications. Experimental and clinical endocrinology & diabetes : official journal, German Society of Endocrinology [and] German Diabetes Association *120*, 184-185.

Tennessen, J.M., Barry, W.E., Cox, J., and Thummel, C.S. (2014). Methods for studying metabolism in Drosophila. Methods *68*, 105-115.

Thummel, C.S. (2001). Molecular mechanisms of developmental timing in C. elegans and Drosophila. Developmental cell *1*, 453-465.

Veenstra, J.A., Agricola, H.J., and Sellami, A. (2008). Regulatory peptides in fruit fly midgut. Cell and tissue research *334*, 499-516.

Verhage, M., McMahon, H.T., Ghijsen, W.E., Boomsma, F., Scholten, G., Wiegant, V.M., and Nicholls, D.G. (1991). Differential release of amino acids, neuropeptides, and catecholamines from isolated nerve terminals. Neuron *6*, 517-524.

Xie, L., Zhu, D., and Gaisano, H.Y. (2012). Role of mammalian homologue of Caenorhabditis elegans unc-13-1 (Munc13-1) in the recruitment of newcomer insulin granules in both first and second phases of glucose-stimulated insulin secretion in mouse islets. Diabetologia *55*, 2693-2702.

Yan, L.J. (2014). Pathogenesis of chronic hyperglycemia: from reductive stress to oxidative stress. Journal of diabetes research *2014*, 137919.

Yu, L., McPhee, C.K., Zheng, L., Mardones, G.A., Rong, Y., Peng, J., Mi, N., Zhao, Y., Liu, Z., Wan, F., *et al.* (2010). Termination of autophagy and reformation of lysosomes regulated by mTOR. Nature *465*, 942-946.

Zhang, H., Liu, J., Li, C.R., Momen, B., Kohanski, R.A., and Pick, L. (2009). Deletion of Drosophila insulin-like peptides causes growth defects and metabolic abnormalities. Proceedings of the National Academy of Sciences of the United States of America *106*, 19617-19622.

APPENDIX: Individual contributions to this work

Jung Kim performed the experiments. Jung Kim & Thomas P. Neufeld designed and interpreted experiments and wrote the manuscript.